Updating the estimation of age and growth of bigeye tuna (*Thunnus obesus*) in the Indian Ocean from counts of daily and annual increments in otoliths.

Paige Eveson[1] Patricia L. Luque[2] Jessica Farley[1], Kyne Krusic-Golub[3], Iraide Artetxe-Arrate[2], Naomi Clear[1], Igaratza Fraile[2], Antoine Duparc[4], Caroline Faucheux[4], Maria Jose Juan-Jorda[5], Anne-France Mattlet[6], Adriana Maria Nunes Alves[7], Ricardo Jorge Silva Sousa[7], Alexandra CSG. Guerreiro[8], Constance Diaha[9], Hilario Murua[10], Iker Zudaire[2]

[1] CSIRO Environment, Hobart, Australia; paige.eveson@csiro.au

[2] AZTI, Marine Research, Basque Research and Technology Alliance (BRTA), Pasaia, Gipuzkoa, Spain; plastra@azti.es

[3] Fish Ageing Services Pty Ltd, Victoria, Australia; kyne.krusicgolub@fishageingservices.com

[4] IRD, UMR MARBEC, Sète, France;

[5] IEO-CSIC, AGENCIA ESTATAL CONSEJO SUPERIOR DE INVESTIGACIONES CIENTÍFICAS, Calle Serrano, 117. 28006 Madrid, SPAIN

[6] EUROPECHE, ASSOCIATION DES ORGANISATIONS NATIONALES D'ENTREPRISES DE PECHE DE L'UE, Rue Montoyer, 24. 1000 Bruxelles, BELGIUM;

[7] DRM-MADEIRA, SECRETARIA REGIONAL DE MAR E PESCA, Avenida do Mar e das Comunidades Madeirenses, 23. 9000-050 Funchal, PORTUGAL;

[8] DRP-AÇORES, SECRETARIA REGIONAL DO MAR E DAS PESCAS, Rua Consul Dabney Colonia Alema, Apartado 9. 9900-014 Horta, PORTUGAL;

[9] CRO, CENTRE DE RECHERCHES OCÉANOLOGIQUES, 29, Rue des Pêcheurs. BPV 18 Abidjan, COTE D'IVOIRE;

[10] ISSF, International Seafood Sustainability Foundation, Washington DC, USA; hmurua@iss-foundation.org

Executive summary

This paper provides an update on bigeye tuna (*Thunnus obesus*) (BET) otolith ageing activities in the western Indian Ocean that have occurred since Farley et al. (2021). New age estimates were obtained for 146 bigeye tuna ranging in size from 22.0 to 182.5 cm fork length (FL), using a combination of both daily (n=42) and annual (n=104) ageing methods. The youngest fish was aged 59 days and the oldest was 11.6 years. These new data were combined with age data obtained during the 'GERUNDIO' project[1] (Farley et al. 2021), providing a total of 253 age estimates for analysis. Three growth models were fit to the age and length data (von Bertalanffy (VB), Richards, and VB log k). The two-phase VB log k model provided a better fit to the data for very small fish (< ~40 cm FL) and thus, is our preferred model for BET in the study area; however, all three models gave very similar fits above 40 cm (~age 0.4 years). Overall, our analysis shows that growth is rapid in the first few years with fish reaching ~60 cm FL at age 1 year and ~85 cm FL at age 2 years. Mean asymptotic length was estimated to be 170.8 cm FL, slightly higher than estimated in Farley et al. (2021). The length-at-otolith weight data (which is independent of the age estimation method) showed a change in otolith growth at ~40 cm FL, which is consistent with the length-at-age data and lends support to the 2-stage VB model (i.e., a transition between two growth phases, from fast growth up to ~40 cm FL followed by slower growth). The models presented here are quite different from the growth model of Eveson et al. (2012), which was used as the base scenario in the 2022 assessment. The Eveson et al. (2012) model was estimated using primarily tag-recapture data. Investigations done by Eveson & Farley (2021) (included as Appendix B to this paper for convenience), and further follow-up investigations, showed that the release ages estimated for tagged fish within the Eveson et al. (2012) model were being estimated incorrectly due to the two tagged cohorts having very different growth rates, and thus different mean lengths at age. As such, we recommend no longer using the Eveson et al. (2012) model, but instead using one of the growth models presented in this study in future stock assessments. The updated data analysis in the current study indicates that males reach slightly larger sizes, on average, than females (mean asymptotic length of 171.7 cm FL for males compared to 164.4 cm for females). Although the estimated differences in growth between sexes were relatively small, further exploration of sex-specific growth dynamics may provide valuable insights and is encouraged in future assessments. Furthermore, we continue to recommend that additional otoliths are collected and aged, particularly in the eastern regions of the Indian Ocean and from BET >180 cm FL, to provide further information on growth and longevity of BET at the oceanic basin scale. These data will be useful for assessing whether there are regional differences in growth and may also provide information regarding inter-annual variation in growth. Preliminary age validation/verification work using otoliths and data from the IOTTP (Farley et al. 2021) provides evidence that the otolith ageing method used in this study is accurate. However, we recommend that further age validation work is undertaken.

[1] Collection and analysis of biological samples of tropical tunas, swordfish, and blue shark to improve age, growth and reproduction data for the Indian Ocean Tuna Commission (IOTC), FAO Contract No. 2020/SEY/FIDTD/IOTC - CPA 345335.

1. Introduction

Bigeye tuna (*Thunnus obesus*) (BET) is a highly migratory species that inhabits the epipelagic zone of tropical and subtropical waters of the three major oceans, from latitudes of approximately 45°N to 45°S (see Appendix 2, from IOTC–2022–WPTT24–R[E). Their spawning areas are restricted to environments with warm sea surface temperatures (>20°C) and mesoscale oceanographic activity (Kim and Na, 2022). BET represents an important source of nourishment and livelihood for numerous nations around the world. It is also a significant component of the global fisheries market, being among the top 10 most fished marine species. As such, this species experiences significant fishing pressure, with total catches reaching about 94,803 tonnes in 2021 in the Indian Ocean (Appendix 2, from IOTC–2022).

In the Indian Ocean, BET is considered to be a single biological stock, based on genetic studies that indicate no evidence of intra-oceanic genetic differentiation within the Indian Ocean (Chiang et al. 2008; IOTC 2019; Davies et al. 2020; Diaz-Arce et al. 2020) and tagging studies that have demonstrated large-scale movements of Bigeye Tuna within the Indian Ocean (IOTC 2014).

In 2022, a stock assessment was carried out for bigeye tuna in the IOTC area of competence to update the 2019 stock assessment, which determined the BET stock is overfished and subject to overfishing. The spawning stock biomass in 2021 (SB2021) was estimated to be 25% (80% CI: 23-27%) of the unfished levels and 90% (75-105%) of the level that can support MSY. Fishing mortality (F) was estimated at 1.43 (80%CI: 1.1-1.77) times the FMSY level. Hence, the assessment indicates that SB2021 is below SBMSY and F2021 is above FMSY (79%) (IOTC–2022–WPTT24–R[E).

An integral part of developing stock assessment models is to have a sound understanding of growth (Maunder and Piner 2015; Methot and Wetzel 2013). Growth models are used in stock assessments to convert length measurements of the catch to age measurements, and to model biomass and fishing processes over time (Murua et al. 2017). Therefore, accurate and updated age and growth parameters are required for robust stock assessments and management advice. The age and growth of bigeye tuna has been investigated widely in the Atlantic (Paccico et al. 2023) and the Pacific (Farley et al., 2017, 2020) and more scarcely in the Indian Oceans (Eveson et al. 2012, 2015; Farley et al. 2021).

In 2020, the European Union and the Indian Ocean Tuna Commission (IOTC) supported the 'GERUNDIO' project for the "*collection and analysis of biological samples of tropical tunas, swordfish, and blue sharks to improve age, growth and reproduction data for the IOTC*". As part of that project, biological samples were collected from the western part of the IOTC assessment region and analysed along with existing samples from previous research initiatives to provide preliminary otolith-based age (daily and annual) and growth estimates for bigeye tuna (Farley et al. 2021). In addition, age validation work for bigeye tuna in the Indian Ocean was undertaken as part of the project by analysing otoliths from fish that had been tagged and recaptured in the IOTTP. Moreover, Farley et al. (2017; 2020) developed a new method to estimate the decimal age of bigeye tuna in the western and central Pacific Ocean from validated counts of daily and annual growth zones in otoliths that was also applied for the first time to estimate age for bigeye tuna from the Indian Ocean (Farley et al. 2021). The preliminary growth curve estimated by Farley et al (2021) was included in the final group of models in the 2022 bigeye tuna stock assessment.

Since the completion of the 'GERUNDIO' project, additional bigeye tuna otoliths that were collected under other projects (i.e., BAOBAB, PROBIO and ITUNNES) have been selected and aged from length classes that were under-represented in the original work (Farley et al. 2021). This paper provides an update on these ageing activities and presents growth models fit to the updated age and length dataset.

2. Methods

2.1. Otolith selection, preparation and reading

Otoliths from 147 bigeye samples collected in the western Indian Ocean from 2021 to 2024 were selected for age estimation based on fish length and sampling location to ensure age estimates were obtained from length classes poorly sampled in previous work and considering sex information across the spatial range of fish sampled. Otoliths from 42 small fish (22.0-63.8 cm FL) were selected for daily ageing and otoliths from 105 fish (73.0-182.5 cm FL) were selected for annual ageing. The sagittal otoliths were cleaned, dried, and weighed to the nearest 0.0001 g if complete. The otoliths were prepared and read following the methods described in Farley et al. (2021) and outlined below.

Daily ageing

Otoliths selected for daily age reading were prepared as either (i) single longitudinal (frontal) sections from the primordium to the postrostral axis of the otolith through the primordium following Schaefer and Fuller (2006), or (ii) single transverse sections through the primordium following Williams et al. (2013). Transverse sections were prepared for small fish (<35 cm FL) and longitudinal sections for larger fish, as previous work for yellowfin tuna in the Indian Ocean showed that estimates of age were consistent between preparation methods for fish <42 cm FL (Farley et al. 2023). Transverse sections were preferred for small fish because (i) otoliths from very small fish are much easier to prepare as transverse sections and (ii) transverse sections have the advantage that direct measurements of the otolith growth required for the daily-age-otolith size relationship for the decimal age calculation (see section 2.2 below) can be taken from the same sample prepared for age estimation. Given that juvenile yellowfin and bigeye growth is likely to be different for this study we chose 35 cm as the cut off length as a precaution.

The number of visible micro-increments (assumed daily growth zones) were counted from the primordium to the terminal edge of the section under high magnification on a compound microscope. All otoliths were prepared and read by Fish Ageing Services Pty Ltd (FAS) in Australia. Each sample was read twice by the same reader and if the difference in counts was >10%, then a third reading was completed. The average of the two closest readings was used as the final count.

The distance from the primordium to the terminal edge of the otolith was measured on all transversely prepared otoliths. For the otoliths prepared longitudinally, the second otolith of the pair was selected and prepared in the transverse section following methods used for preparing tuna otoliths for annual ageing (Anon, 2002) to allow for the measurement of otolith growth as described above.

Annual ageing

Otoliths selected for annual age reading were prepared as multiple transverse sections following the methods outlined in Anon (2002). All otoliths were prepared and read by the same experienced reader at FAS that read all samples in Farley et al. (2021).

An image analysis system was used to read the sectioned otoliths via a dissecting microscope and transmitted light. The system counts and measures the distance of each manually marked opaque zone from the primordium and collects an annotated image from each sample read. The opaque zones at the terminal edge of the otolith were only marked if they were complete and some translucent material was evident after the opaque zone. The otolith edge was classified as new opaque, narrow translucent or wide translucent based on the criteria developed for Pacific bigeye tuna otoliths (Farley et al. 2017) and each reading was assigned a confidence score of 0-5 (poor-good). All samples were initially read twice and a third time if the first two estimates disagreed either by zone count or edge type. Intra-reader ageing error was determined using the first two readings. Average percent error (Beamish and Fournier 1981) and age difference tables were used to assess the precision of the readings.

2.2. Decimal (annual) age calculation

Decimal age was calculated for each fish with an annual count based on the method developed for bigeye and yellowfin tunas (*Thunnus albacares*) in the western Pacific Ocean (Farley et al. 2020). The decimal ages for bigeye tuna in Farley et al. (2021) were also re-calculated because the datasets used in the calculation were updated with additional data from the current study, plus the methods were revised slightly. Decimal age was calculated using three steps:

First, the age of each fish when the first opaque zone was completed in the transverse section was calculated. This was done using the updated data set of daily age and otolith size measurements from transverse sectioned otoliths. The updated daily age-otolith size relationship was estimated using a power curve (Append Figure 1).

Second, the number of complete annual increments in the otolith was calculated. A complete annual increment is one opaque zone + one translucent zone, which represents presumably one year of growth, and is calculated as the total count of opaque zones minus 1.

Third, the time elapsed after the last counted opaque zone was deposited and when the fish was caught was estimated using the width of the marginal increment in the otolith as a proportion of the expected width of the complete annulus for that age class. Expected increment width was obtained by fitting an exponential decline relationship between age class and the annual increment width measurements for all fish examined for annual ageing[2] (see Append Figure 2).

The total age of each fish was estimated by adding together the age components estimated in each step. Note that for otoliths with zero or one opaque zones (within the range of the power curve in Append Figure 1), age was estimated using only the otolith measurement (i.e., only step 1).

2.3. Growth analysis

Three different growth models were fit to the age and length data for bigeye: (1) von Bertalanffy (1938) (VB); (2) Richards (1959); (3) von Bertalanffy with a logistic growth rate parameter (VB log k) (Laslett et al. 2002). Age estimates from both the daily counts and the annual counts after applying the decimal age algorithm were included in the models.

The VB growth model has the form:

$$L_a = L_\infty(1 - e^{-k(a-a_0)})$$

where L_a is the fork length at age a, L_∞ is the mean asymptotic length, k is a relative growth rate parameter (year^{-1}), and a_0 is the age at which fish have a theoretical length of zero. We fit the model using maximum likelihood estimation assuming a Gaussian error structure with mean 0 and variance σ^2.

The Richards model can be expressed in different ways, but here we used the following parameterisation:

$$L_a = L_\infty(1 - {}^{1}/_{b}\, e^{-k(a-a^*)})^b$$

where L_∞ and k are defined as for the VB model, a^* determines the point of inflection and b governs the shape of the curve. Note that when b = 1, the Richards equation is equivalent to the VB equation.

The VB log k model (Eveson et al. 2012; 2015) has the form:

$$L_a = L_\infty \left\{ 1 - e^{-k_2(a-a_0)} \left(\frac{1 + e^{-\beta(a-a_0-\alpha)}}{1 + e^{\alpha\beta}} \right)^{-\frac{(k_2-k_1)}{\beta}} \right\}$$

where this function allows for a change in growth from a VB curve with growth rate parameter k_1 to a VB curve with growth rate parameter k_2. There is a smooth transition between the two stages governed by a logistic function, where α governs the age at which the midpoint of the transition occurs and β governs the rate of the transition (being sharper for larger values).

[2] In Farley et al. (2021), the expected increment width for a given age class was calculated as the empirical mean increment width from the otolith measurements taken routinely from the otoliths included in annual ageing. Here, we have revised to use the expected value from a fitted relationship between age class and increment width, which should be more robust for age classes without much data.

To fit these models, we used maximum likelihood estimation assuming a Gaussian error structure with mean 0 and variance σ^2. Akaike's information criterion (AIC) (Akaike 1974) and plots of residuals were used to compare the fits.

In addition, sex-specific VB growth models were fit to the data. Only a VB model was used since the data when broken down by sex were insufficient to achieve convergence with the more complex VB log k model. Almost all the new age data for adults comes from fish caught in the north-west Indian Ocean; thus, the spatial distribution of samples in the updated age-length dataset still does not allow for us to fit area-specific growth models.

3. Results

3.1. Daily and annual age estimates

Age estimates were obtained from all 42 otoliths selected for daily ageing. Age ranged from 59 to 410 days. Age estimated from transverse sections for fish 32-35 cm FL overlapped well with the estimates from the longitudinal 36-38 cm FL which indicates that age estimates using transverse sections <35cm FL is good for BET from the Indian Ocean.

Counts of opaque zones were obtained for 104 of the 105 otoliths selected for annual ageing (one was missing its tip). The counts ranged from 1 to 11 years. Figure 1 is an example of an otolith prepared for annual ageing with the (assumed) annual opaque zones marked.

These data were combined with the daily and annual age data from Farley et al. (2021), providing a combined total of 79 daily age estimates and 174 annual age estimates for growth analysis. Decimal age estimates from the combined dataset (including daily and annual estimates) ranged from 0.13 to 14.7 years.

Figure 1. Transverse preparation of a bigeye tuna otolith prepared for annual reading showing presumed annual opaque zones indicated with white circles. Sample IM-23-BAOBAB-530 (302_039_072), fork length 152 cm. Aged as 7 completed zones with an opaque edge.

3.2. Growth analysis

A total of 253 age-length data points were included in the growth model (174 decimal annual age estimates and 79 daily age estimates). Figure 2 shows the locations where bigeye tuna otoliths used in the growth models were collected, and Figure 3 shows the length frequency of fish included in the analysis broken down by sex.

All three growth curves (VB, Richards and VB log k) provided similar fits (Figure 4A); however, the two-phase VB log k model gave the most parsimonious fit according to AIC (Table 1) and the best fit to small fish (< ~40 cm FL) (Figure 4B). The VB log k model indicates there is a transition between two VB growth phases around age 0.4 years (~40 cm), with a high growth rate parameter in the first phase (k_1=0.9) followed by a lower growth rate parameter in the second phase (k_2=0.28) (Table 1).

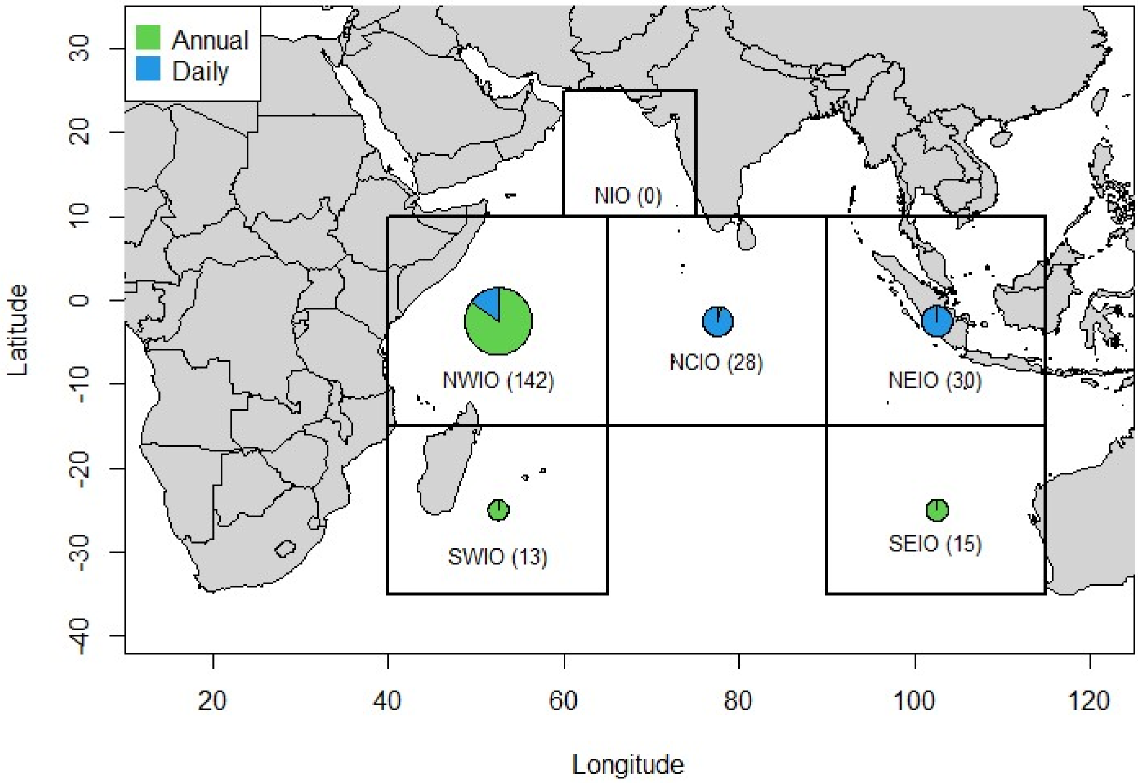

Figure 2. Map showing sample locations of bigeye tuna included in the growth analysis (note that the location for 25 samples was unknown, so these are not shown on the map). Circle size is proportional to total sample size (given in parentheses), with segments indicating annual (green) and daily (blue) age estimates. NIO = north Indian Ocean, NWIO = northwest Indian Ocean, SWIO = southwest Indian Ocean, NCIO = north central Indian Ocean, NEIO = northeast Indian Ocean, SEIO = southeast Indian Ocean

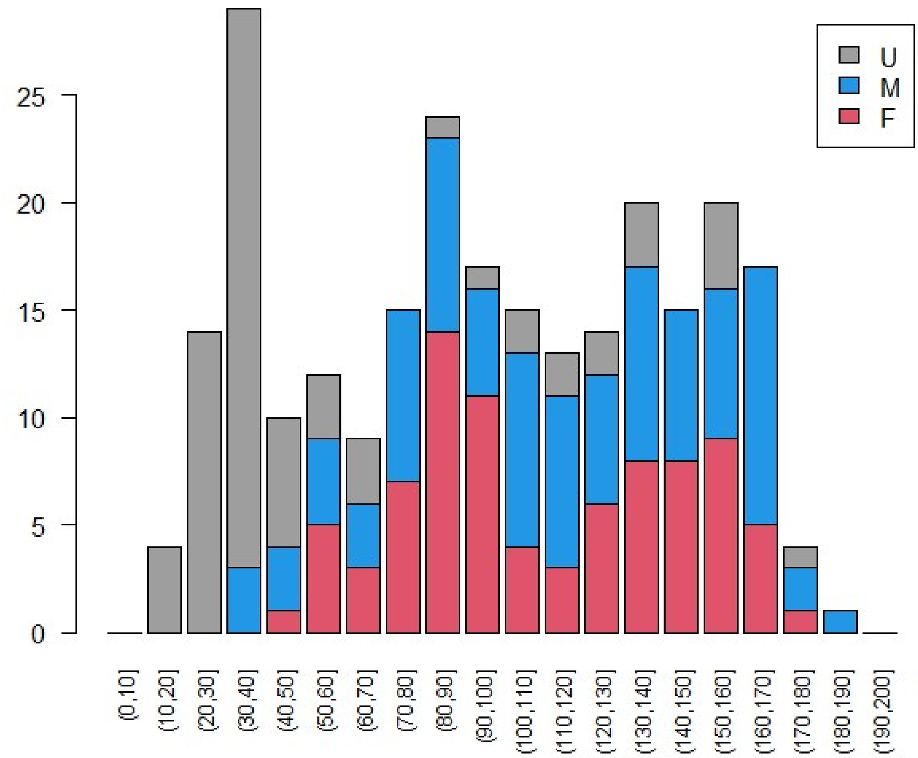

Figure 3. Length frequency (fork length, 10-cm length bins) of bigeye tuna included in the growth analysis (n=253). F = female, M = male, U = unknown sex.

(A)

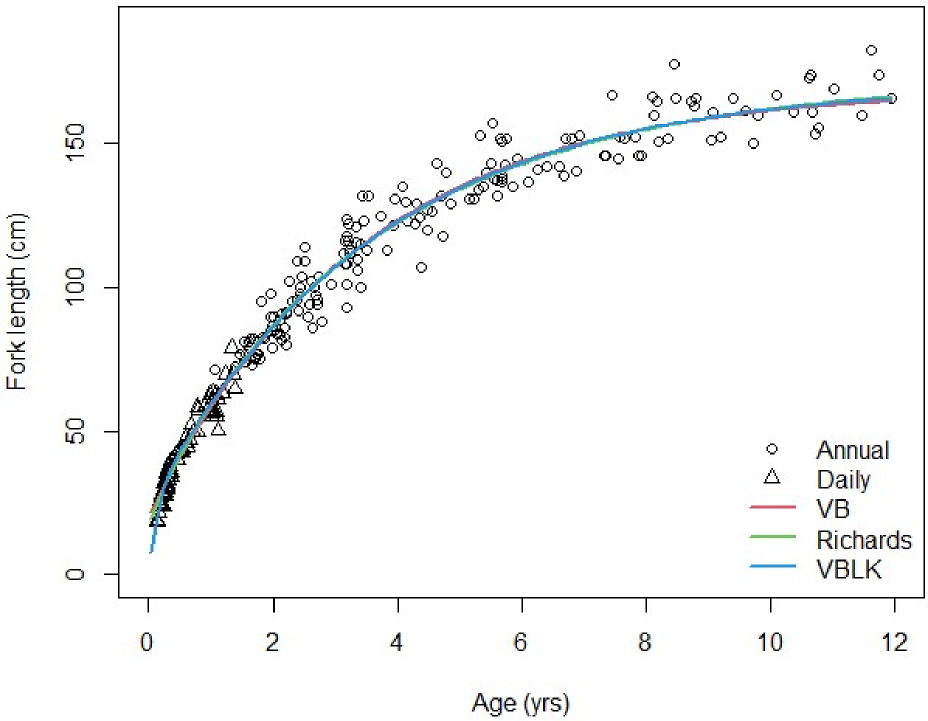

(B)

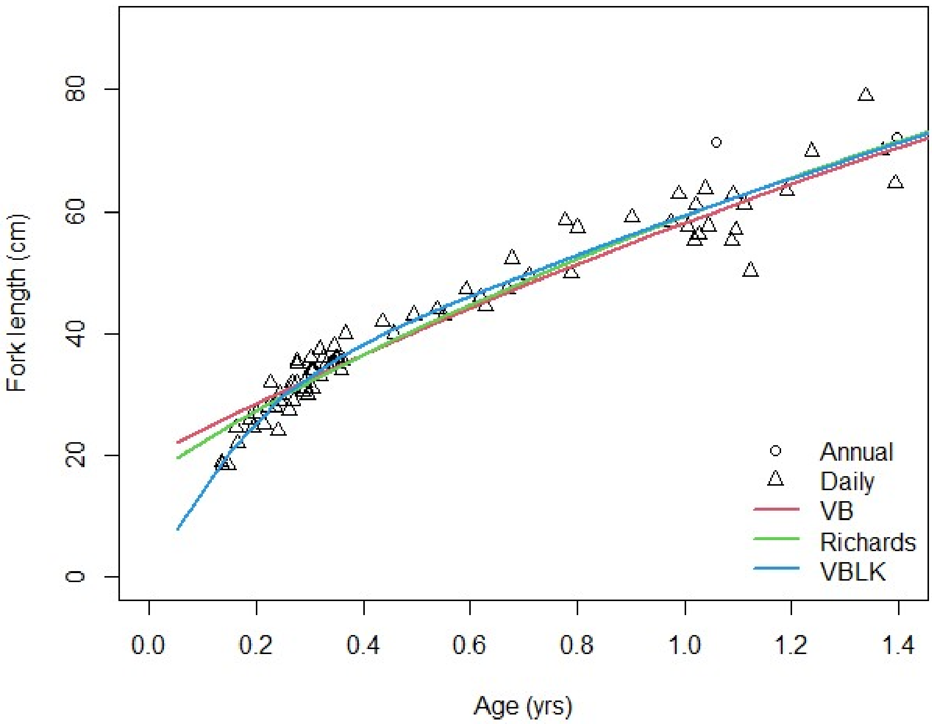

Figure 4. (A) Length-at-age data (daily and annual) for bigeye tuna with von Bertalanffy (VB), Richards and VB log k (VBLK) growth models fit to the data. (B) A close-up of the length-at-age data and growth curves for small/young bigeye tuna.

Table 1. Parameter estimates from fitting von Bertalanffy (VB), Richards and VB log k growth models to the bigeye tuna length at age data (n=253). Standard errors for the parameter estimates are given in parentheses.

Model	L_∞	k/k_1	k_2	α	$b/\beta/\tau$	a_0/a^*	σ	AIC
VB	169.2 (1.6)	0.30 (0.01)	--	--	--	-0.42 (0.03)	6.68 (0.30)	1687.1
Richards	172.7 (2.8)	0.25 (0.02)	--	--	0.81 (0.08)	-1.05 (0.40)	6.64 (0.30)	1686.1
VB log k	170.8 (1.9)	0.90 (2.9)	0.28 (0.01)	0.23 (1.0)	13.8 (33.0)	-0.004 (0.28)	6.56 (0.29)	1683.9

Since otolith weight (independent of the ageing method) may be an indicator of age, we examined the otolith weight to fish length relationship for a larger number of samples (n=369) than were aged (n=253), to ascertain if the otolith growth was consistent with the observed fish growth. The results show a similar pattern in growth, with a transition at ~40 cm FL from a fast-growing phase to a slower-growing phase (Figure 5).

Preliminary data analysis indicated that males grow slightly faster and reach slightly larger sizes, on average, than females (Figure 6, Table 2). Recall that a VB model was used to fit the sex-specific models since the data were insufficient to achieve convergence with a VB log k model. There is some indication that males grow slightly larger in the length-at-otolith weight data as well (Figure 5).

The length-at-age data were insufficient in some regions to model region-specific growth within the Indian Ocean. There is perhaps some indication in the length-at-age data that bigeye tuna in the western Indian Ocean grow slightly slower than those in the eastern Indian Ocean, but the sample size in the east (particularly for adult fish, which all come from the south-east) is too small to draw any conclusions and other factors such as size-selective fishing could bias the data (Figure 7).

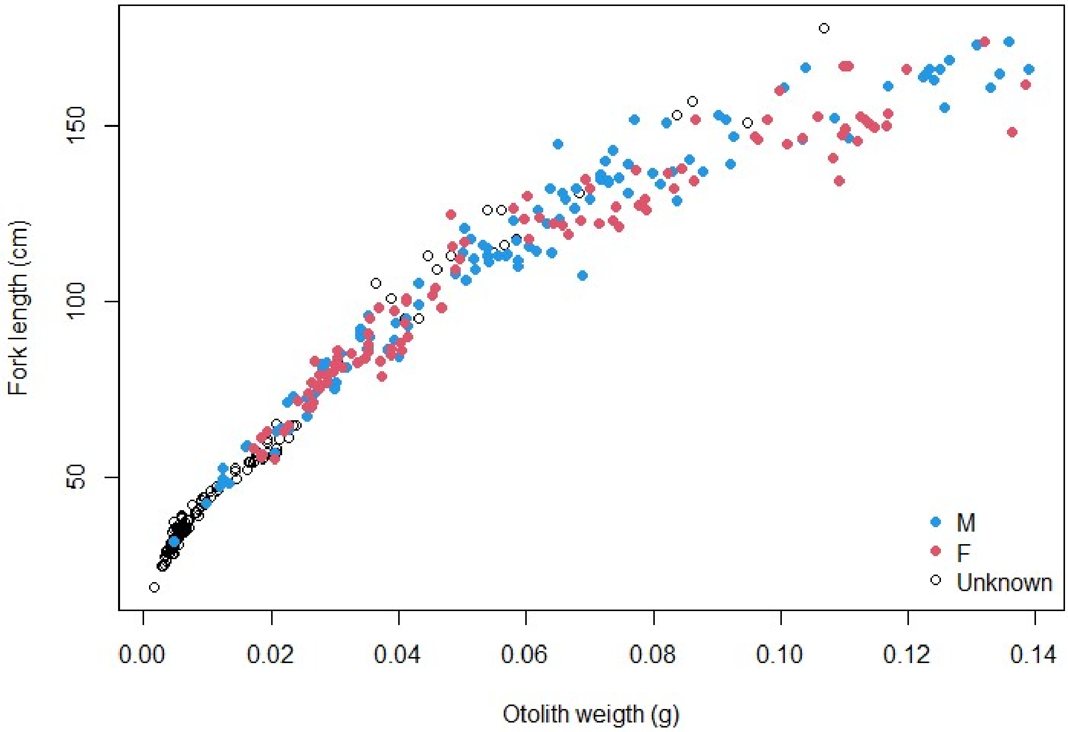

Figure 5. Relationship between otolith weight and fork length for bigeye tuna in the Indian Ocean by sex (n=369). M = male, F = female.

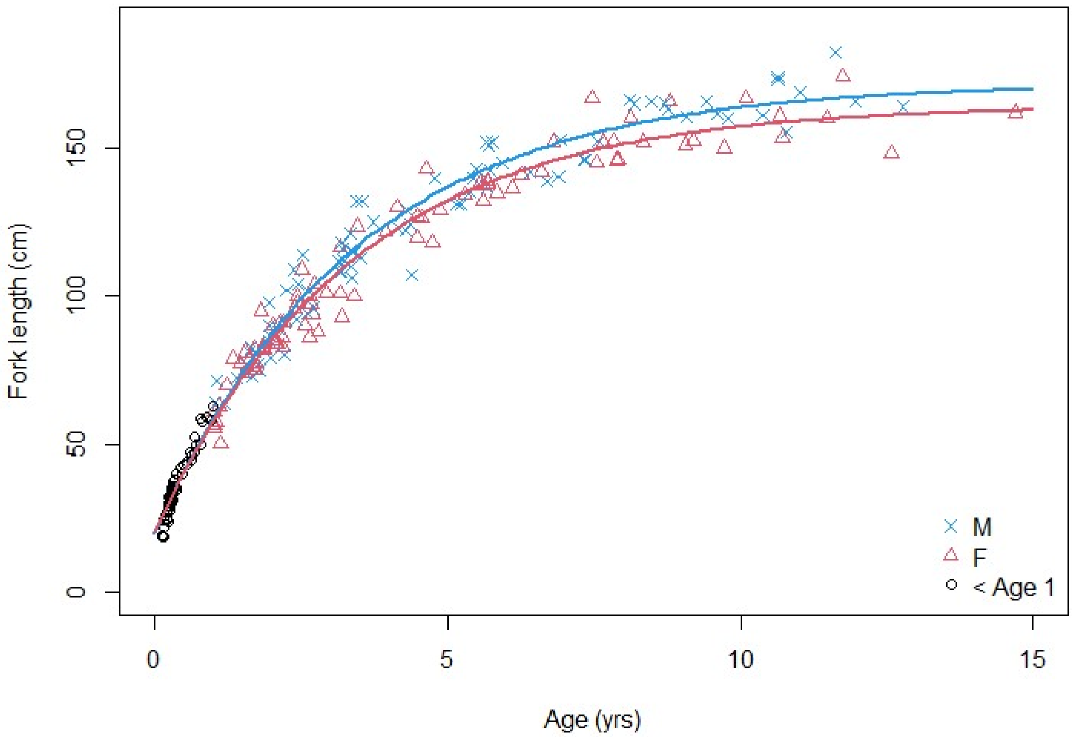

Figure 6. Length-at-age data by sex for bigeye tuna in the Indian Ocean, with VB growth models fitted to the data for each sex (M = male, F = female). Note that fish with age < 1 are included in the models for both sexes.

Table 2. Parameter estimates from fitting a von Bertalanffy (VB) growth model to sex-specific bigeye tuna length at age data. Note that YOY fish (age < 1 year) (n=63) are included in the models for both sexes. Standard errors for the parameter estimates are given in parentheses.

Model	Sex	*n*	L_∞	*k*	a_0	σ
VB	**F**	146	164.4 (1.9)	0.30 (0.01)	-0.43 (0.03)	5.58 (0.33)
VB	**M**	148	171.7 (2.0)	0.29 (0.01)	-0.42 (0.03)	5.73 (0.33)

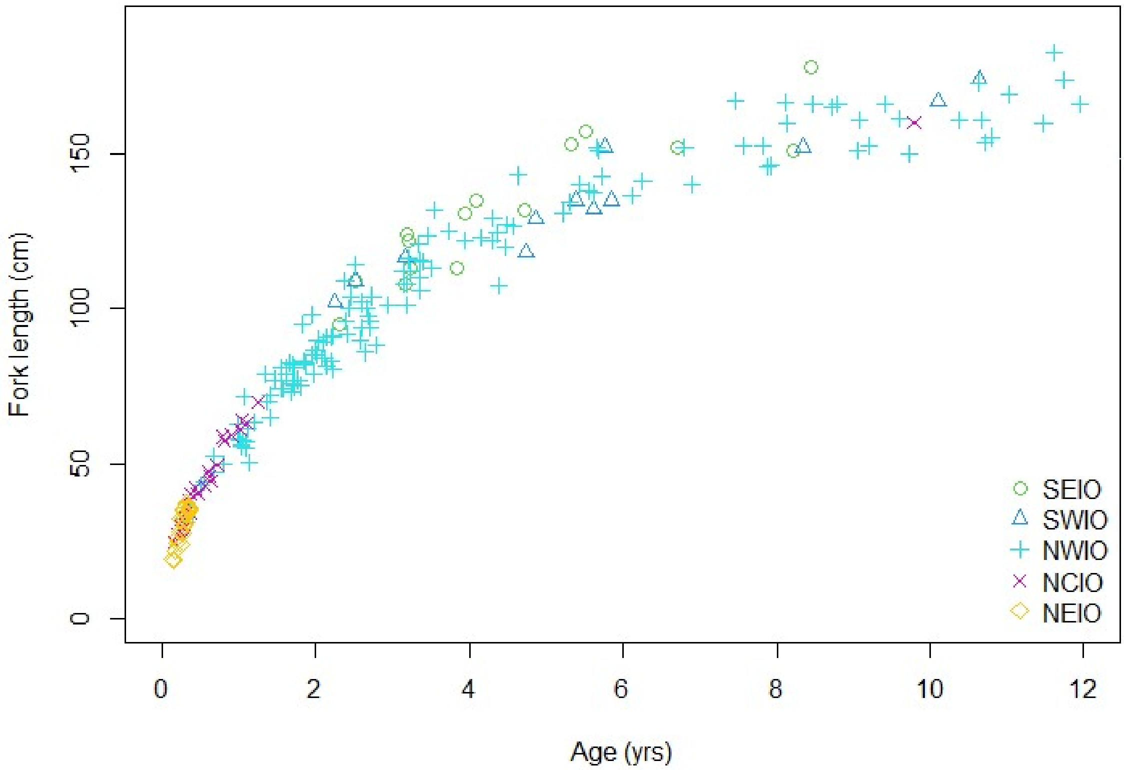

Figure 7. Length-at-age data by area for bigeye tuna caught in the Indian Ocean (n=228, noting that sample location is unknown for 25 samples). See Figure 2 for definition of regions.

4. Discussion

This study builds on the work of Farley et al. (2021), which estimated the decimal age of BET in the Indian Ocean using counts of daily and annual growth zones in sectioned otoliths. Here, we obtained additional age estimates, which combined with those from Farley et al. (2021), resulted in a dataset of 253 age estimates from BET ranging in FL from 18.5 to 182.5 cm. The combined decimal age estimates span from 0.13 to 14.7 years. Although comprehensive age validation work for BET in the Indian Ocean has yet to be completed, preliminary analyses by Farley et al. (2021) using otoliths and data from the IOTTP support the accuracy of the ageing method used in this study. Furthermore, our comparisons between the annual and daily age estimates showed strong concordance (see Figure 6), providing additional confidence in the validity of our method for calculating decimal age.

Among the growth models tested, the two-stage von Bertalanffy (VB) model provided the best fit to the length-at-age data, particularly for fish smaller than ~40 cm FL. Additionally, patterns in the length-at-otolith weight data—independent of the ageing method—were similar to those in the length-at-age data, lending further support to the two-stage VB model. Our findings indicate that BET tuna grow rapidly in the early years, reaching approximately ~60 cm FL by age one and ~85 cm FL by age two. The estimated mean asymptotic length ($L\infty$) was estimated around 170.8 cm FL, with a maximum observed age of over 14 years, slightly higher than estimated in Farley et al. (2021). Similarly, a study of bigeye tuna age and growth from the eastern Indian Ocean estimated the oldest fish to be 15 years old (Wujdi et al, 2023).

The estimation of Amax is particularly important, as it directly influences the estimation of natural mortality (M), a key parameter in stock assessment models. Underestimating maximum age can lead to overestimation of natural mortality, which in turn may bias estimates of stock productivity and reference points. Therefore, the identification of older individuals in this study not only supports the validity of the ageing method but also contributes to more accurate and biologically realistic estimates of natural mortality for BET. These results underscore the value of incorporating direct ageing techniques and flexible growth models into stock assessment frameworks. Doing so enhances the precision of life-history parameter estimates and supports more informed and precautionary fisheries management.

Growth patterns for males and females were similar up to two to three years of age. Beyond this point, males exhibited a slightly greater average length-at-age than females, with mean $L\infty$ estimates of 171 cm and 164 cm FL, respectively.

The updated VB log k growth model presented in this paper is very similar to the VB log k model in Farley et al. (2021), which was included in the final group of models in the 2022 bigeye tuna stock assessment. These models are quite different from the growth model of Eveson et al. (2012), which was used as the base scenario in the 2022 assessment. The Eveson et al. (2012) model was estimated using tag-recapture data (IOTTP; Murua et al. 2015) and otolith-based daily age estimates (Sardenne et al. 2015), but the tagging data were most influential. Investigations done by Eveson & Farley (2021) (included as Appendix B for convenience), and further follow-up investigations, showed that the release ages estimated for the tagging data in the Eveson et al. (2012) model (estimated using random effects) were being estimated incorrectly due to two cohorts with very different growth rates, and thus different mean lengths at age, being tagged and released. As such, we recommend using one of the growth models presented here (noting that the VB log k, VB and Richards models all gave very similar fits) as the base growth model in future stock assessments. Although the estimated difference in growth between sexes was relatively small, it may still be valuable to investigate the potential effects of sex-specific growth in future assessments. While the current dataset does not reveal clear regional differences in growth, limited sample sizes in certain areas prevent definitive conclusions. We continue to recommend increased otolith collection from the eastern Indian Ocean, where sample sizes remain low, particularly for adult fish. Ageing these additional otoliths will improve our understanding of regional growth and longevity patterns and help evaluate the potential for inter-annual variation in length-at-age to influence growth curve estimation.

Acknowledgements

The otolith collection used from this study was obtained from PROBIO (Contract no. 00001-INP2021-33), GERUNDIO (Contract no. 2020/SEY/FIDTD/IOTC - CPA 345335), PSTBS-IO (GCP/INT/233/EC), BAOBAB (OF-IM-23-499A), EMOTION (Project ANR-11-JSV7-007), IOTTP, and ITUNNES (101157296 — EMFAF-2023-PIA-FisheriesScientificAdvice) projects. The views expressed herein can in no way be taken to reflect their official opinion of the funding agencies. We thank the many vessel owners, skippers, crews, and processors who provided fish for sampling. Authors want to thank to all the observers, port samplers and coordinators for collecting, storing and transporting otoliths across the Indian Ocean. Authors want to thank to the many people who were involved in the collection of otoliths used in this study; Iñigo Krug, Iñigo Onandia, Deniz Kukul, Naiara Serrano, Lluis Horrach and Arnaitz Mugerza (AZTI-BRTA). We also thank Admir Sutrovic, Graham Porter and Christine Rees (FAS) for preparing and or weighing the otoliths.

References

Anon (2002). A Manual for Age Determination of Southern Bluefin *Thunnus maccoyii*. Otolith Sampling, Preparation and Interpretation. Available at: http://www.ccsbt.org/userfiles/file/docs_english/meetings/meeting_reports/ccsbt_09/report_of_daews.pdf/

Appleyard, S.A., Ward, R.D. and Grewe, P.M. 2002. Genetic stock structure of Bigeye Tuna in the Indian Ocean using mitochondrial DNA and microsatellites. Journal of Fish Biology 60: 767-770.

Beamish, R.J. and Fournier, D.A. (1981). A method for comparing the precision of a set of age determinations. Canadian Journal of Fisheries and Aquatic Sciences 38: 982–983. doi: 10.1139/f81-132.

Campana, S.E. (1992). Measurement and interpretation of the microstructure of fish otoliths. In Otolith Microstructure Examination and Analysis'. Ed. by D. K. Stevenson, and S. E. Campana. Canadian Special Publication of Fisheries and Aquatic Sciences 117: 59–71.

Cayré, P., Diouf, T. (1984). Croissance du thon obese (Thunnus obesus) de l'Atlantique d'apres les resultats de marquage. Madrid, International Commission for the Conservation of Atlantic Tunas (ICCAT). Rec.Doc. Sci. 20(1), 180-187.

Chiang, H-C, Hsu, C-C, Wu, GC-C, Chang, S-K and Yang, H-Y (2008). Population structure of bigeye tuna (*Thunnus obesus*) in the Indian Ocean inferred from mitochondrial DNA. Fisheries Research, 90: 305–312.

Collette, B.B., Boustany, A., Fox, W., Graves, J., Juan Jorda, M. & Restrepo, V. (2021). *Thunnus obesus*. The IUCN Red List of Threatened Species 2021: e.T21859A46912402. https://dx.doi.org/10.2305/IUCN.UK.2021-2.RLTS.T21859A46912402.en

Davies, C., Marsac, F., Murua, H., Fahmi, Z., Fraile, I. (2020). Summary of population structure of IOTC species from PSTBS-IO project and recommended priorities for future work. IOTC-2020-SC23-11_Rev1, 16p.

Díaz-Arce, N., Grewe, P., Krug, I Artetxe, I., Ruiz, J., et al. (2020). Evidence of connectivity of bigeye tuna (*Thunnus obesus*) throughout the Indian Ocean inferred from genome-wide genetic markers. IOTC-2020-WPTT22(AS)-16.

Eveson, P., Million, J., Sardenne, F., Le Croizier, G. (2012). Updated growth estimates for skipjack, yellowfin and bigeye tuna in the Indian Ocean using the most recent tag-recapture and otolith data. IOTC-2012-WPTT14-23.

Eveson, P., Million, J., Sardenne, F., Le Croizier, G. (2015). Estimating growth of tropical tunas in the Indian Ocean using tag-recapture data and otolith-based age estimates. Fisheries Research 163: 58–68.

Eveson, P., and Farley, J. (2021) Investigating growth information for yellowfin and bigeye tuna from the IOTTP tag-recapture data. IOTC-2021-WPTT23-21.

Farley, J. H., Clear, N. P., Leroy, B., Davis, T. L. O., McPherson, G. (2006). Age, growth and preliminary estimates of maturity of bigeye tuna, *Thunnus obesus*, in the Australian region. Marine and Freshwater Research, 57: 713–724.

Farley, J., Eveson, P., Krusic-Golub, K., Clear, N., Sanchez, C., Roupsard, F., Satoh, K., Smith, N., Hampton, J. (2018). Update on age and growth of bigeye tuna in the WCPO: WCPFC Project 81. WCPFC-SC14-2018/ SA-WP-01.

Farley, J., Eveson, P., Krusic-Golub, K., Kopf, K. (2021a). Southwest Pacific Striped Marlin Population Biology (Project 99). WCPFC-SC17-2021/SA-IP-11.

Farley, J., Eveson, P., Krusic-Golub, K., Sanchez, C., Roupsard, F., McKechnie, S., Nicol, S., Leroy, B., Smith, N., Chang, S.-K. (2017). Project 35: Age, growth and maturity of bigeye tuna in the western and central Pacific Ocean. WCPFC-SC13-2017/ SA-WP-01.

Farley, J., Krusic-Golub, K., Eveson, P. (2021b). Updating age and growth parameters for South Pacific albacore (Project 106). WCPFC-SC17-2021/SA-IP-10.

Farley, J., Krusic-Golub, K., Eveson, P., Clear, N., Rouspard, F., Sanchez, C., Nicol, S., and Hampton, J. (2020). Age and growth of yellowfin and bigeye tuna in the western and central Pacific Ocean from otoliths. WCPFC-SC16-2020/SC16-SA-WP-02.

Farley, J., Krusic-Golub, K., Eveson, P., Luque, P.L., Fraile, I., Artetxe-Arrate, I., Zudaire, I., Romanov, E., Shahid, U., Razzaque, S., Parker, D., Clear, N., Murua, H., Marsac, F., Merino, G. (2023). Estimating the age and growth of yellowfin tuna (*Thunnus albacares*) in the Indian Ocean using otoliths. IOTC-2023-WPTT25-20

Fu, D. (2019). Preliminary Indian Ocean bigeye stock assessment 1950-2018 (Stock Synthesis). IOTC–2019–WPTT21–61.

Gaertner, D., Hallier, J.P. (2009). An updated analysis of tag-shedding by tropical tunas in the Indian Ocean. IOTC-2009-WPTT-34.

Hallier, J.P., Stequert, B., Maury, O., and Bard, F.-X. (2005). Growth of bigeye tuna (*Thunnus obesus*) in the eastern Atlantic Ocean from tagging-recapture data and otolith readings. Col. Vol. Pap. ICCAT 57: 181–194.

IOTC (2020). Report of the 22nd Session of the IOTC Working Party on Tropical Tunas, Stock Assessment Meeting. OTC–2020–WPTT22(AS)–R[E]_Rev1.

Kim, J., & Na, H. (2022). Interannual variability of yellowfin tuna (Thunnus albacares) and bigeye tuna (Thunnus obesus) catches in the southwestern Tropical Indian Ocean and its relationship to climate variability. *Frontiers in Marine Science*, *9*, 857405.

Langley, A., Herrera, M., & Million, J. (2009). Updated stock assessment for bigeye tuna in the Indian Ocean up to 2008 using Stock Synthesis III (SS3). IOTC–2009–WPTT–20. Indian Ocean Tuna Commission, Working Party on Tropical Tunas, 11th Session

Laslett, G.M., Eveson, J.P., Polacheck, T. (2002). A flexible maximum likelihood approach for fitting growth curves to tag-recapture data. Can. J. Fish. Aquat. Sci. 59, 976–986.

Lehodey, P., Leroy, B. (1999) Age and growth of yellowfin tuna (*Thunnus albacares*) from the western and central Pacific Ocean as indicated by daily growth increments and tagging data. Working paper YFT-2, 12th meeting of the Standing Committee on Tuna and Billfish, Tahiti.

Maunder, M.N., Crone, P.R., Valero, J.L., Semmens, B.X. (2015). Growth: theory, estimation, and application in fishery stock assessment models CAPAM Workshop Series Report 2 March 2015.

Murua, H., Eveson, J.P., Marsac, F. (2015). The Indian Ocean Tuna Tagging Programme: Building better science for more sustainability. Fish. Res. 163:1-6.

Murua, H., Rodrıguez-Marin, E., Neilson, J., Farley, J., Juan-Jorda, M.J. (2017) Fast versus slow growing tuna species – age, growth, and implications for population dynamics and fisheries management. Rev. Fish Biol. Fish DOI 10.1007/s11160-017-9474-1

R Core Team (2021). R: A language and environment for statistical computing. R Foundation for Statistical Computing, Vienna, Austria. URL https://www.R-project.org/.

Sardenne, F., Dortel, E., Le Croizier, G., Million, J., Labonne, M., Leroy, B., Bodin, N., Chassot, E. (2015) Determining the age of tropical tunas in the Indian Ocean from otolith microstructures. Fish. Res. 163:44–57. doi:10.1016/j.fishres.2014.03.008

Schaefer, K.M., Fuller, D.W., 2006. Estimates of age and growth of bigeye tuna (Thunnus obesus) in the eastern Pacific Ocean, based on otolith increments and tagging data. IATTC Bulletin 23, 35–59.

Stéquert, B., Conrad, F. 2004. Age and growth of bigeye (*Thunnus obesus*) in the western Indian Ocean. Cybium 28(2): 163-170.

Williams AJ, Farley JH, Hoyle SD, Davies CR, Nicol SJ (2012) Spatial and sex-specific variation in growth of albacore tuna (*Thunnus alalonga*) across the South Pacific Ocean. PLoS ONE 7(6): e39318. doi:10.1371/journal.pone.0039318.

Wright, P.J., Panfili, J., Morales-Nin, B., Geffen, A.J. (2002). Types of calcified structures. In: Manual of fish Sclerochronology. (Eds J Panfili, HD Pontual, H Troadec, PJ Wright.) pp. 31–57. (Ifremer-IRD coedition: Brest, France).

Wujdi, A., Nugroho, S. C., Zedta, R. R., Hartaty, H., Putri, M. R. A., Rochman, F., Tampubolon, P. A. R., Kurniawan, R., Pramurdya, Y. N., & Setyadji, B. (2023). Age and Growth estimation of Bigeye Tuna, Thunnus obesus (Lowe, 1839) in the Eastern Indian Ocean Deduced from Otolith Microstructure. HAYATI Journal of Biosciences, 30(4), 670–681. https://doi.org/10.4308/hjb.30.4.670-681

Appendix A – Otolith data for decimal age algorithm

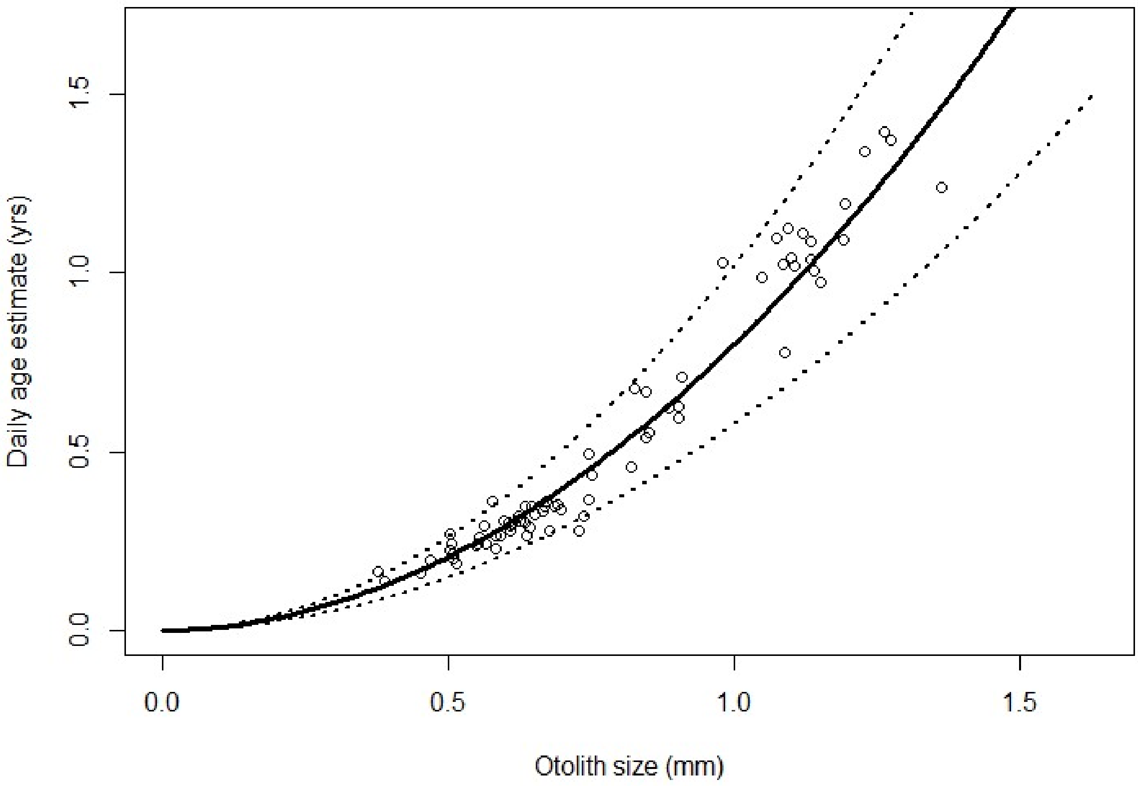

Append Figure 1. Relationship between otolith size (mm) and daily age (yrs) with fitted power curve for bigeye tuna (dashed lines show approximate 95% confidence bounds). Otolith size is the distance from the primordium to the edge in transverse sectioned otoliths.

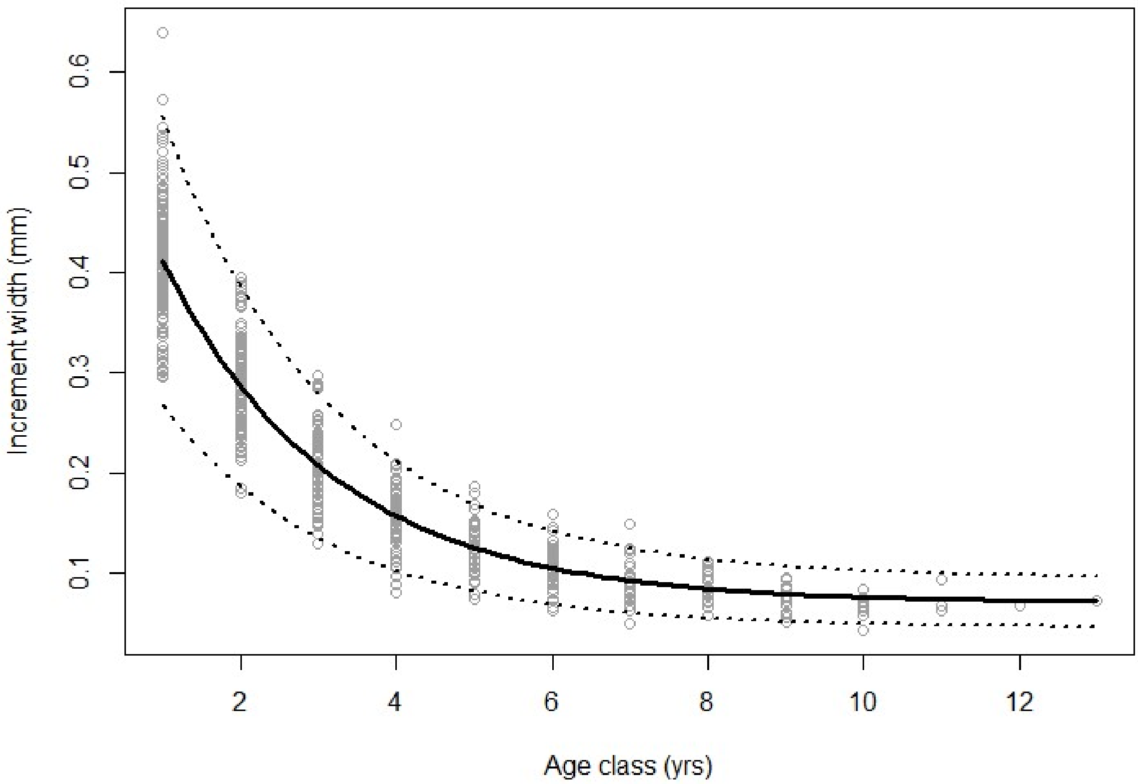

Append Figure 2. Relationship between age class (yrs) and increment width (mm) for bigeye tuna, with fitted exponential decline curve (dashed lines show approximate 95% confidence bounds).

Appendix B – Copy of IOTC-2021-WPTT23-21

Investigating growth information for yellowfin and bigeye tuna from the IOTTP tag-recapture data

Paige Eveson and Jessica Farley

CSIRO Oceans and Atmosphere, Hobart, Australia; paige.eveson@csiro.au

Executive summary

Previous growth models that were estimated for yellowfin (*Thunnus albacares*) and bigeye (*T. obesus*) tuna using tag-recapture data from the Indian Ocean Tuna Tagging Programme (IOTTP) suggested both species have a phase of slow growth as juveniles, followed by a phase of faster growth (Eveson et al. 2015; Dortel et al. 2015). One of the drawbacks of using tag-recapture data to model growth is that the age of a fish at release is unknown. These models deal with the problem by modelling the age at release as a random effect.

In 2020, the European Union and the Indian Ocean Tuna Commission (IOTC) supported a project to develop new estimates of age and growth for yellowfin and bigeye tuna in the Indian Ocean. The aim was to follow methods recently developed by Farley et al. (2017; 2020) for bigeye tuna in the Western Central Pacific Ocean (WCPO) to estimate the age and growth of yellowfin and bigeye tuna from counts of daily and annual growth zones in otoliths. Using the relationship between the daily age estimates obtained from this project and fish length, the age at release for fish in the tag-recapture data could be estimated from their release lengths. The resulting age estimates are very different than those obtained from the random effects models. Here we present these new findings and discuss potential reasons for the differences.

Introduction

A large-scale tagging programme, known as the Regional Tuna Tagging Project of the Indian Ocean (RTTP-IO), was initiated in 2005 to address uncertainties in growth, as well as other key inputs to the stock assessments, for yellowfin (YFT; *Thunnus albacares*), bigeye (BET; *T. obesus*) and skipjack (SKJ; *Katsuwonus pelamis*) tuna in the Indian Ocean. As part of the RTTP-IO, large numbers of all three species were tagged in the western Indian Ocean, primarily off Tanzania, between May 2005 and August 2007. Additional tagging also occurred in the eastern Indian Ocean as part of small-scale tagging operations, including extensive tagging of SKJ and YFT off the Maldives in 2004 and 2007-2009. In total, over

63,000 YFT, 35,000 BET, and 100,000 SKJ were tagged as part of the RTTP-IO and small-scale tagging operations, collectively known as the Indian Ocean Tuna Tagging Programme (IOTTP). Recaptures occurred subsequently in commercial fisheries operating in the Indian Ocean. At the time of data compilation for the Indian Ocean Tuna Tagging Symposium in 2012, the percent of tag returns was approximately 16% for each of the three species. Details of the tagging and recovery operations can be found in Hallier (2008) and Hallier and Fonteneau (2015).

In our investigation here, we concentrate only on the tag-recapture data from YFT and BET. For both species, the growth rates calculated from the tag-recapture data (cm/day) show a clear change/increase at ~55 cm fork length, with smaller fish growing more slowly than larger fish (Eveson et al. 2015). The magnitude of the change is larger for YFT. Daily age estimates from otoliths collected as part of the IOTTP (Sardenne et al. 2015) lent some support to this pattern, but discrepancies in age estimates between different otolith readers and large variability in the resulting length at age data made any conclusions difficult (Eveson et al. 2015).

One of the drawbacks of using tag-recapture data to model growth is that the age of a fish at release is unknown. Maximum likelihood and Bayesian approaches have been developed that deal with this by modelling the age at release as a random variable (e.g., Palmer et al., 1991; Wang et al., 1995; Laslett et al., 2002; Dortel et al. 2015). These models attempt to estimate a release age distribution that is most consistent with the release length, recapture length and time at liberty data for the growth model being assumed. For example, if a von Bertalanffy model is chosen, the assumption is that growth rates decline with age, so for fish of a given length, those with a lower growth rate will be estimated to be older than those with a higher growth rate.

Eveson et al. (2015) used tag-recapture data from the IOTTP along with otolith daily age estimates from Sardenne et al. (2015) to estimate growth models for YFT and BET. For both species, a VB log k growth curve (Laslett et al. 2002) was chosen to capture the two phases of growth. The fitted growth models suggest YFT and BET have a phase of slower growth when they are juveniles, followed by a phase of faster growth. YFT make a quick transition between growth phases, with a short period of very rapid growth immediately following the age of transition, whereas BET make a smoother, more gradual transition. Kolody (2011) suggested that differential size-selectivity between the FAD (fish aggregating device) and free-set components of the purse seine fishery could result in apparent two-stanza growth; however, the pattern held when recaptures from either component of the fishery were considered independently.

In 2020, the European Union and the Indian Ocean Tuna Commission (IOTC) supported the 'GERUNDIO' project for the "*collection and analysis of biological samples of tropical tunas, swordfish, and blue sharks to improve age, growth and reproduction data for the IOTC*". One of the objectives of the project was to develop new estimates of age and growth for yellowfin and bigeye tuna in the Indian Ocean. The aim was to follow methods recently developed by Farley et al. (2017; 2020) for bigeye tuna in the Western Central Pacific Ocean (WCPO) to estimate the age and growth of yellowfin and bigeye tuna from counts of daily and annual growth zones in otoliths. The results for YFT and BET are presented in Farley et al. (2021a) and Farley et al. (2021b) respectively. Using the relationship between fish length and the daily age estimates obtained from the GERUNDIO study, we could estimate age at release for fish in the tag-recapture data from their release lengths. The resulting age estimates are very different than those obtained from the random effects models in Eveson et al. (2015). Here we present these new findings and discuss potential reasons for the differences.

Methods and Results

In the investigations done here, we used the same tag-recapture data set used in the growth models of Eveson et al. (2015), which had been filtered based on screening criteria determined by the Secretariat of the Indian Ocean Tuna Commission (IOTC).

Yellowfin tuna

Figure 1 shows the release and recapture distributions for YFT, broken down by those released off Tanzania (N=4035) and those released elsewhere (N=301). The distribution of release lengths shows two distinct modes, one centred around 48 cm and the other around 62 cm with a separation between them at ~54 cm (**Figure 2**). The average growth rate for each fish over the time it was at liberty was calculated as the difference between the recapture length and the release length (in cm) divided by the time at liberty (in days). Plotting growth rate against release length shows that fish in the smaller release length mode (<54 cm) had slower growth in general than fish in the larger release length model (≥54 cm) (**Figure 3**). For fish with release lengths ≥54 cm, growth rates decline with length and are also slightly lower for fish at liberty for longer (**Figure 3**), both of which are expected if growth monotonically declines with age (like a von Bertalanffy curve). However, for fish with release length <54 cm, there are two clouds of points, one with slightly higher growth rates than the other. The cloud of fish with higher growth rates corresponds to fish that were at liberty for over a year (**Figure 3**), which suggests the growth of fish released when small (<54 cm) is slow for the first year after tagging, then increases if they remain at liberty for longer, resulting in a higher average growth rate. Another way of looking at these data is to plot growth rate against time at liberty (**Figure 4**). Fish <54 cm at release grow slowly if they were at liberty for less than a year, but the average growth rate starts to increase for fish at liberty longer to a peak around 500-600 days before declining again (as expected as fish get older) (**Figure 4**, top). For fish ≥54 cm at release, there is an initial period of highly variable growth between 100-200 days at liberty, with slow growth for many fish, but for fish at liberty longer than this, their growth rates follow the expected pattern of fast initial growth with a decline over time (**Figure 4**, bottom).

In Farley et al. (2021a), age estimates were obtained for 74 YFT otoliths selected for daily ageing. The relationship between fork length and daily age is shown in **Figure 5**. A non-parametric smooth was fit to these data and used to estimate the age at release of fish in the tag-recapture dataset based on their length at release. Note that age was only estimated for fish with a release length between 20-70 cm (N=4052 out of 4336), since this is the range that was used in developing the age-length relationship. The estimated release ages ranged from 0.24 to 1.21 years with a mean of 0.93 years (**Figure 6**, blue bars). The age at recapture could then be estimated for each fish by summing its estimated release age with the time it was at liberty. A plot of recapture length versus estimated recapture age shows that, up to a recapture age of around 2.5 years, fish released at a smaller size (<54 cm) attained a smaller length at recapture than fish of the same age released at a larger size (≥54 cm) (**Figure 7**). For fish that remained at liberty longer and were recaptured at older ages (>2 years), the lengths at recapture for the two release mode groups become similar. The otolith age and length data from Farley et al. (2021a) are overlaid for comparison, including both the daily age estimates and the decimal age estimates derived from annual ageing (**Figure 7**). These data align quite well with the recapture data for fish from the larger release length mode, particularly for fish <2 years old. Between ages 2 and 4 years, YFT from the otolith data set appear to be slightly smaller for the same age as fish from the tag-recapture data set, but since the data were collected from different regions of the Indian Ocean in different years, this could be explained by spatial or temporal differences in growth.

The recapture length versus age data in **Figure 7** look very different to the data from Eveson et al. (2015), regardless of whether the Sardenne et al. (2015) otolith data from reader Team 1 or Team 2 were included in their models (**Figure 8**). The recapture lengths are the same, so the difference is due to the estimated recapture ages, and more specifically to the estimated release ages since in both cases recapture age is the sum of the estimated release age and the time at liberty. The release ages estimated in Eveson et al. (2015) are older and cover a wider age range than those estimated here (**Figure 6**). Reasons for this are discussed in the Discussion.

Bigeye tuna

Figure 9 shows the release and recapture distributions for BET, broken down by those released off Tanzania (N=2922) and those released elsewhere (N=14). As for YFT, the distribution of release lengths shows two distinct modes, centred around 48 and 62 cm with a separation between them at ~55 cm (**Figure 10**). Similar to YFT, fish in the smaller release length mode (<55 cm) had slower growth in general than fish in the larger release length model (≥55 cm) (**Figure 11**). For BET <54 cm, fish at liberty for over a year still have higher growth rates on average than those at liberty less than a year, but the difference is not as great as for YFT (**Figure 11**). This makes sense since the "jump" in growth rates between the smaller and larger release modes is not as great for BET as for YFT; thus, the average growth rate for fish released when small (<55 cm) but at liberty for over a year still increases, but not by as much. Again, this can be seen by plotting growth rate against time at liberty (**Figure 12**). For fish <55 cm, the increase in the average growth rate that occurs around a year at liberty is not as large as for YFT, and the peak occurs at around 450-500 days before declining (**Figure 12**, top). For BET ≥55 cm at release, growth rates are a bit more variable and slower in the initial period but not to the same extent as for YFT; rather their growth rates better follow the expected pattern of fast initial growth with a decline over time (**Figure 12**, bottom).

In Farley et al. (2021b), age estimates were obtained for 37 BET otoliths selected for daily ageing. The relationship between fork length and daily age is shown in **Figure 13**. A power curve was fit to these data and used to estimate the age at release of fish in the tag-recapture dataset based on their length at release. Age was only estimated for fish with a release length between 18-79 cm (N=2914 out of 2936), since this is the range that was used in developing the age-length relationship. The estimated release ages ranged from 0.30 to 1.64 years with a mean of 0.78 years (**Figure 14**, blue bars). Again, age at recapture was estimated for each fish by summing its estimated release age with the time it was at liberty. As for YFT, BET released at a smaller size (<55 cm) attained a smaller length at recapture than fish of the same age that were released at a larger size (≥55 cm), and this trend held for longer for BET (up to ~age 4) (**Figure 15**). For fish that were recaptured beyond age 4, the lengths at recapture for the two release mode groups became similar. The otolith age and length data from Farley et al. (2021b) are overlaid for comparison, including both the daily age estimates and the decimal age estimates derived from annual ageing (**Figure 16**). Similar to YFT, these data align reasonably well with the recapture data for fish from the larger release length mode, and slight differences could be explained by spatial or temporal differences in growth since the otolith data were collected from different regions of the Indian Ocean in different years.

The recapture length versus age data for BET (**Figure 15**) look very different to the data from Eveson et al. (2015) (**Figure 16**), as are the estimated release age distributions (**Figure 14**). However, compared to YFT, the release ages estimated for BET in Eveson et al. (2015) differed more depending on whether otolith data from reader Team 1 or Team 2 were included in the models. The estimates that included Team 1 data were more similar to our estimates, but still showed a wider age range; those that included Team 2 data also showed a wider age range and were much older than our estimates (**Figure 16**).

Discussion

The results presented here suggest quite different growth curves for YFT and BET from the tag-recapture data than those obtained in Eveson et al. (2015); this is due to very different release ages being estimated for the fish. In fitting a growth model to the data, an assumption is that all fish have the same mean length for a given age – there can be variability around the mean, but not different means for different subsets of fish. The independent release age estimates we obtained here suggest that this assumption is not being met – for both YFT and BET, fish from two different release length modes have different mean lengths at age. The only way for the growth models that estimate release age as a random effect, such as that in Eveson et al. (2015), to deal with this is to estimate the age of the fish with the larger lengths to be older. Although our estimates of release age contain some uncertainty, the relationship between fish length and otolith daily age on which they are based is quite good, and the uncertainty will be small compared to the uncertainty in age estimates obtained from the random effect growth models.

The reason for the difference in mean lengths at age for fish from the two release groups is not clear. If the fish were released in different areas or different years then the difference could be due to spatial or temporal difference in growth; however, they were almost all released off Tanzania in the same two years. For YFT, there were ~300 fish in the data set that were released elsewhere and, while the variability in the growth rates were larger for these fish, they showed a similar pattern to those released off Tanzania (**Figure 4**). There were almost no BET in the dataset from non-Tanzanian releases to make an informative comparison (**Figure 12**). One possible explanation is that tagging affected the growth of the fish, and this effect was larger and lasted longer for fish that were smaller when tagged (i.e., those in the smaller release length mode). This is consistent with our observation that fish from the smaller release length mode eventually "caught up" in length to those from the larger release length mode if they were at liberty for long enough.

Acknowledgements

Authors want to thank to the many people who were involved in the collection of otoliths used in this study; Iñigo Krug, Iñigo Onandia, Deniz Kukul, Naiara Serrano, Lluis Horrach and Arnaitz Mugerza (AZTI-BRTA). We also thank Admir Sutrovic, Graham Porter and Christine Rees (FAS) for preparing and or weighing the otoliths. The otolith collection used from this study was obtained from PROBIO (Contract no. 00001-INP2021-33), GERUNDIO (Contract no. 2020/SEY/FIDTD/IOTC - CPA 345335), PSTBS-IO (GCP/INT/233/EC), BAOBAB (OF-IM-23-499A), EMOTION (Projet ANR-11-JSV7-007), IOTTP, and ITUNNES (101157296 — EMFAF-2023-PIA-FisheriesScientificAdvice) projects. The views expressed herein can in no way be taken to reflect their official opinion of the funding agencies. The tuna tagging data analyzed in this study were collected through the Indian Ocean Tuna Tagging Program (IOTTP) under the Regional Tuna Tagging Project of the Indian Ocean funded by the 9th European Development Fund (9.ACP.RSA.005/006) of the European Union, and small-scale tagging projects funded by the European Union and the Government of Japan, such as the West Sumatra Tuna Tagging Project.

References

Dortel, E., Sardenne, F., Bousquet, N., Rivot, E., Million, J., Le Croizier, G., Chassot, E. (2015). An integrated Bayesian modeling approach for the growth of Indian Ocean yellowfin tuna. Fish. Res. 163, 69–84. https://doi.org/10.1016/j.fishres.2014.07.006.

Eveson, P., Million, J., Sardenne, F., Le Croizier, G. (2012). Updated growth estimates for skipjack, yellowfin and bigeye tuna in the Indian Ocean using the most recent tag-recapture and otolith data. IOTC-2012-WPTT14-23.

Eveson, P., Million, J., Sardenne, F., Le Croizier, G. (2015). Estimating growth of tropical tunas in the Indian Ocean using tag-recapture data and otolith-based age estimates. Fisheries Research 163: 58–68.

Farley, J., Krusic-Golub, K., Eveson, P., Luque, P., Clear, N. et al. (2021a). Estimating the age and growth of yellowfin tuna (Thunnus albacares) in the Indian Ocean from counts of daily and annual increments in otoliths. IOTC-2021-WPTT23-05.

Farley, J., Krusic-Golub, K., Eveson, P., Clear, N., Luque, P. et al. (2021b). Estimating the age and growth of bigeye tuna (Thunnus obesus) in the Indian Ocean from counts of daily and annual increments in otoliths. IOTC-2021-WPTT23-18.

Hallier, J.P. (2008). Status of the Indian Ocean Tuna Tagging Programme – RTTP-IO. IOTC-2008-WPTDA-10.

Hallier, J.P., Fonteneau, A. (2015). Tuna aggregation and movement from tagging data: A tuna “hub” in the Indian Ocean. Fish. Res. 163: 34-43.

Kolody, D. (2011). Can length-based selectivity explain the two stage growth curve observed in Indian Ocean YFT and BET? OTC–2011–WPTT13–33.

Laslett, G.M., Eveson, J.P., Polacheck, T. (2002). A flexible maximum likelihood approach for fitting growth curves to tag-recapture data. Can. J. Fish. Aquat. Sci. 59, 976–986.

Palmer, M.J., Phillips, B.F., Smith, G.T., 1991. Application of nonlinear models with random coefficients to growth data. Biometrics 47, 623-635.

Sardenne, F., Dortel, E., Le Croizier, G., Million, J., Labonne, M., Leroy, B., Bodin, N., Chassot, E. (2015) Determining the age of tropical tunas in the Indian Ocean from otolith microstructures. Fish. Res. 163:44–57. doi:10.1016/j.fishres.2014.03.008.

Wang, Y.-G., Thomas, M.R., Somers, I.F., 1995. A maximum likelihood approach for estimating growth from tag-recapture data. Can. J. Fish. Aquat. Sci. 52, 252-259.

Figures – yellowfin tuna

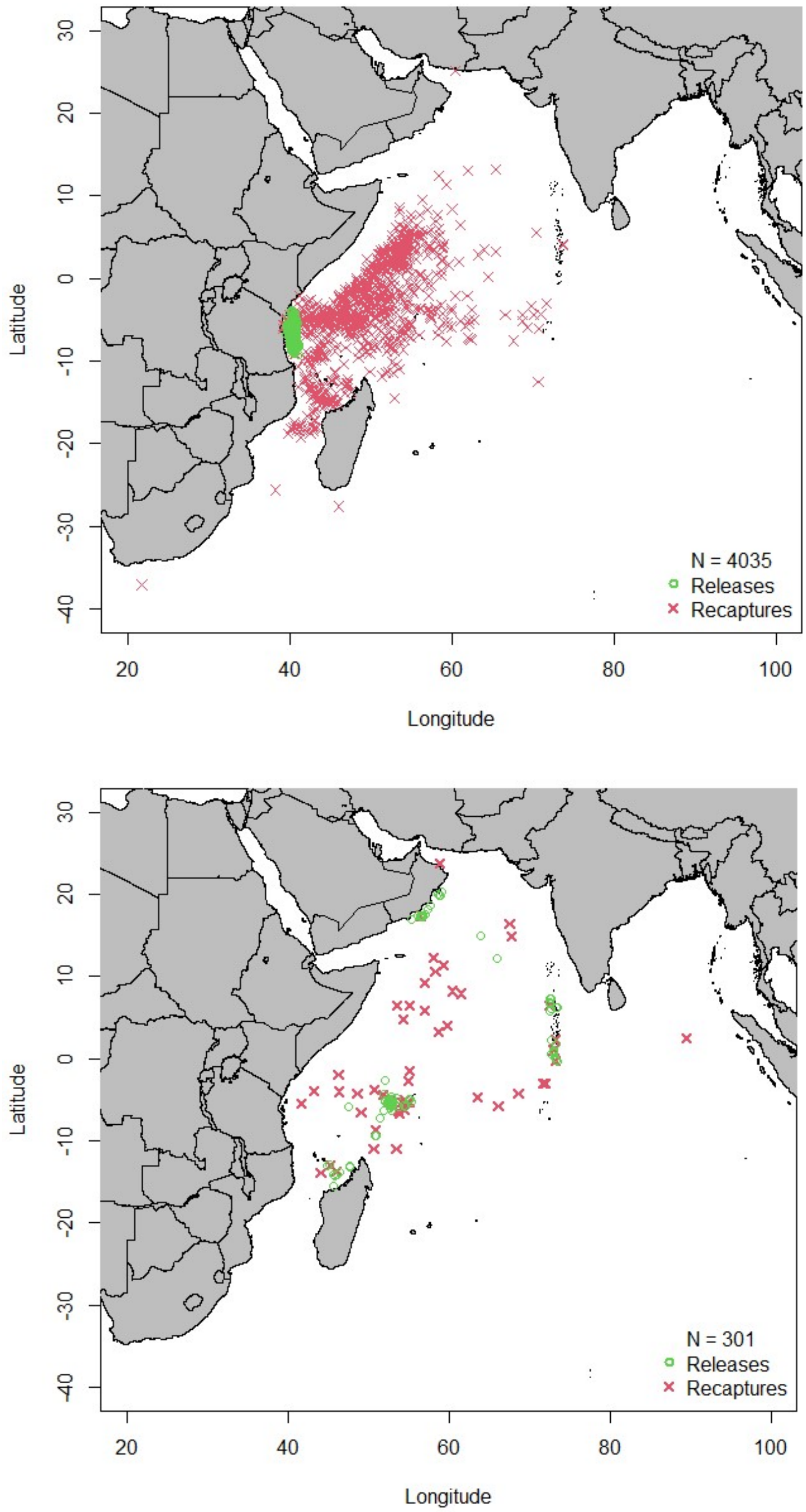

Figure 1. Map of the release and recapture locations for yellowfin tuna used in the growth analysis of Eveson et al. (2015), showing fish that were released off Tanzania (top) and released elsewhere (bottom).

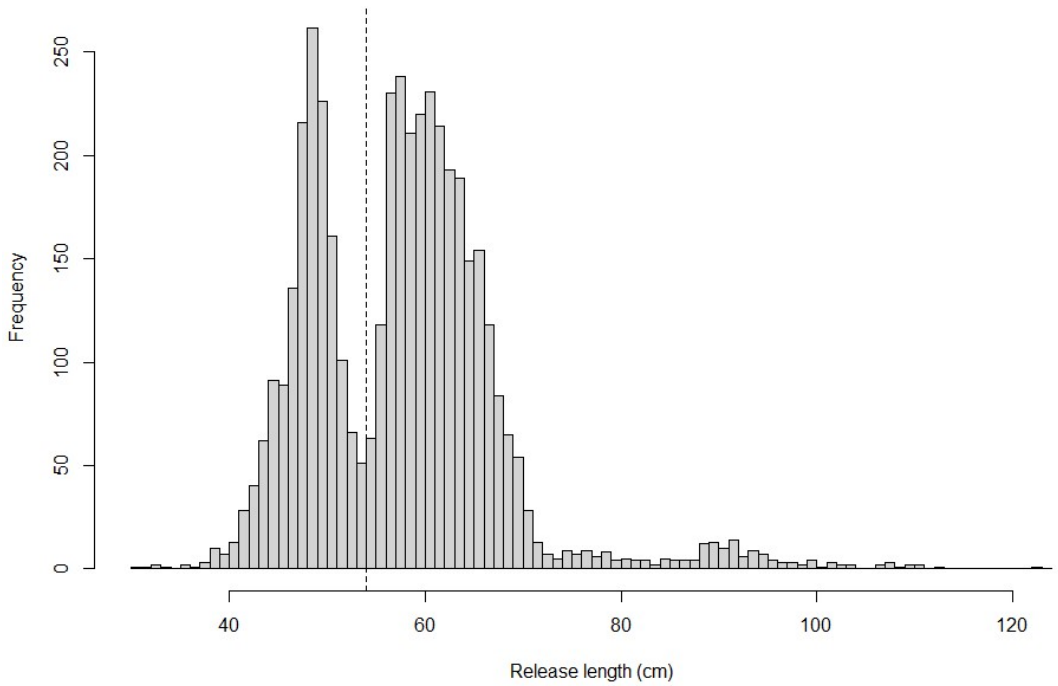

Figure 2. Release length distribution of yellowfin tuna used in the growth analysis of Eveson et al. (2015). There is a separation between modes at 54 cm (dashed vertical line).

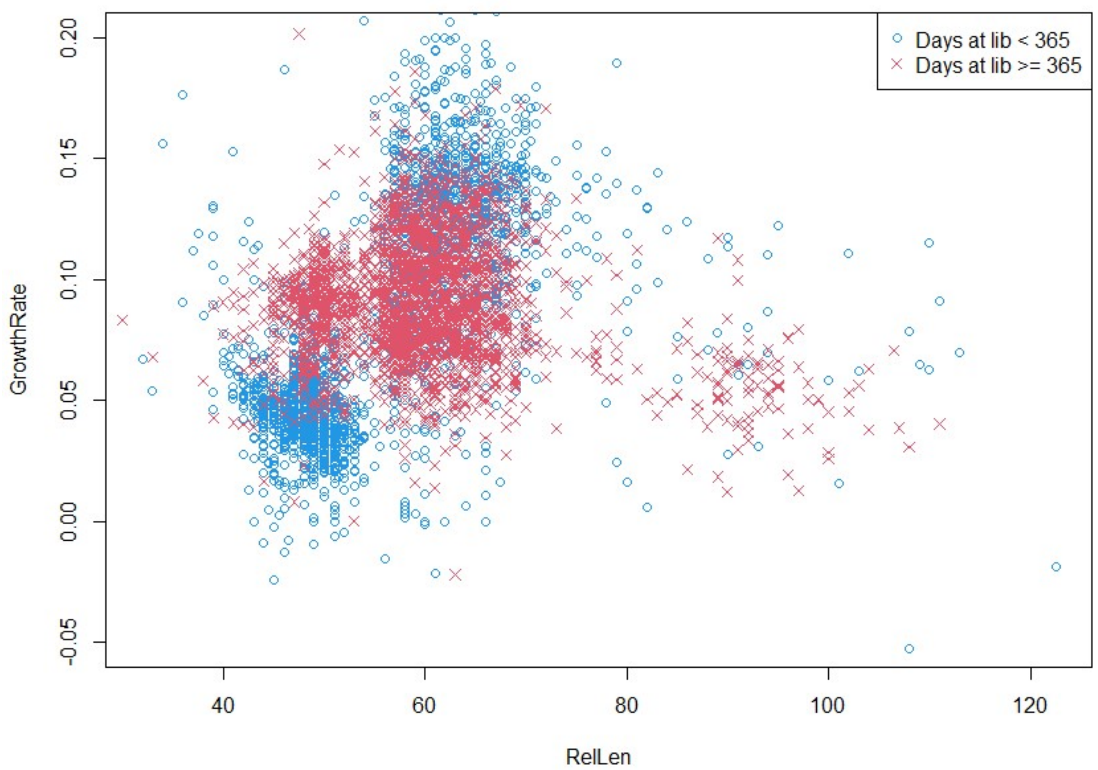

Figure 3. Growth rate (cm/day) versus release length (cm) for yellowfin tuna, broken down by time at liberty (<365 days vs ≥365 days).

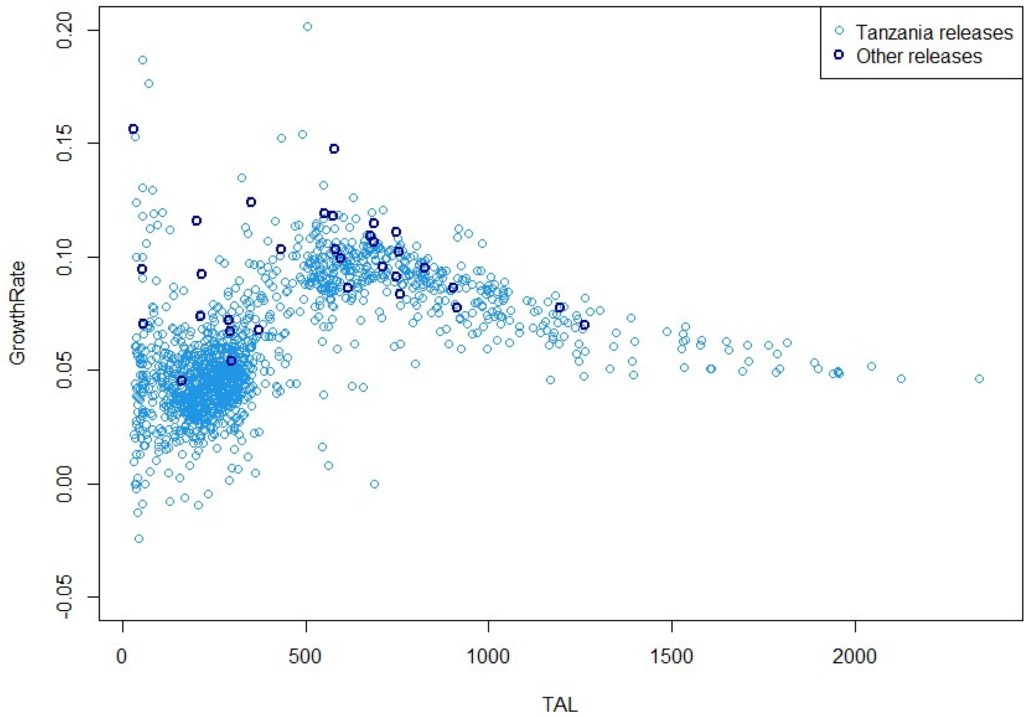

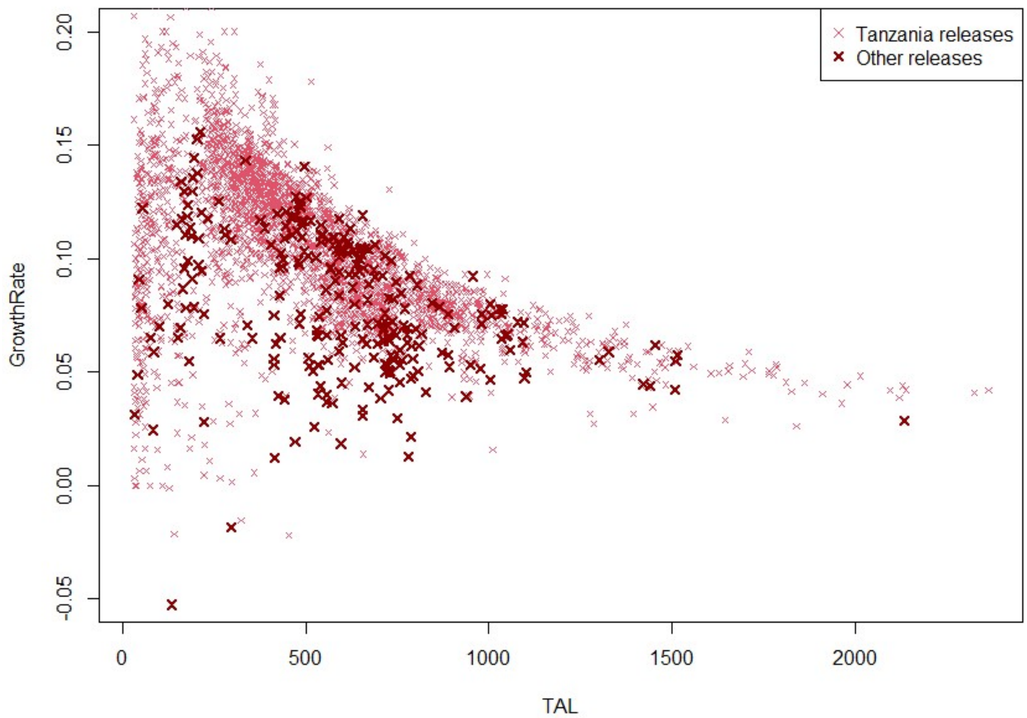

Figure 4. Growth rate (cm/day) verses time at liberty (TAL, days) for yellowfin tuna that were < 54 cm at release (top) and ≥54 cm at release (bottom). Those released in areas other than Tanzania are highlighted for comparison.

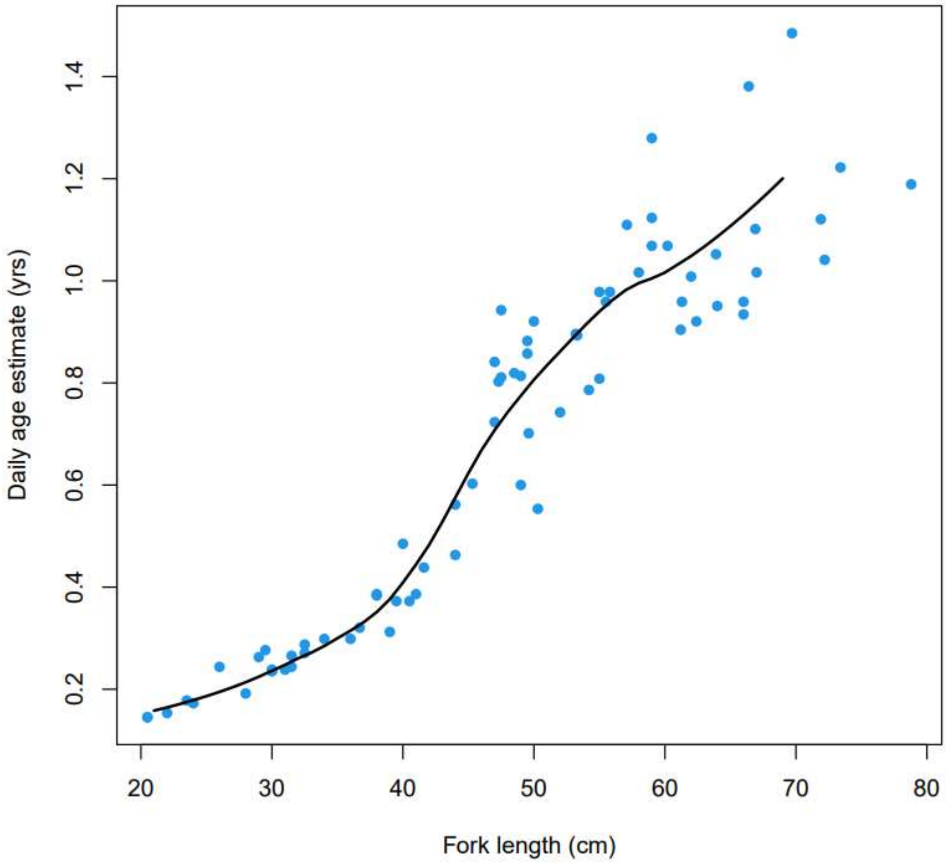

Figure 5. Fork length vs otolith daily age for yellowfin tuna, with a non-parametric smooth model fitted to the data (taken from Farley et al. 2021a). Only fish < 70 cm FL were included in the smooth since the data are too sparse and variable for larger fish to be confident in the age-length relationship.

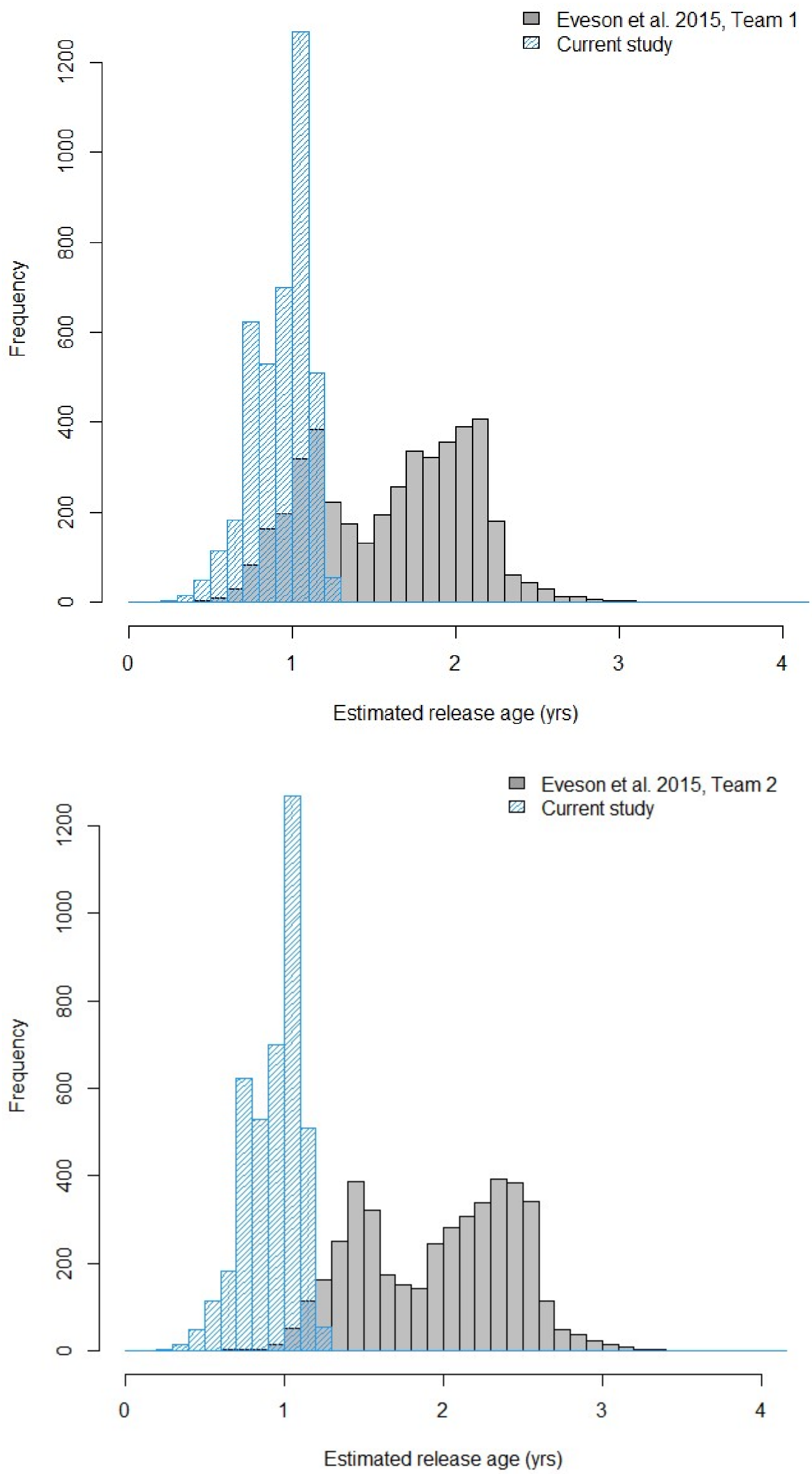

Figure 6. Histogram of release ages estimated for yellowfin tuna in the current study using the length versus daily age relationship in Figure 5 (blue bars) compared to release ages estimated from the growth model in Eveson et al. (2015) (grey bars), which included tag-recapture data and otolith data from Sardenne et al. (2015) for reader Team 1 (top) or reader Team 2 (bottom).

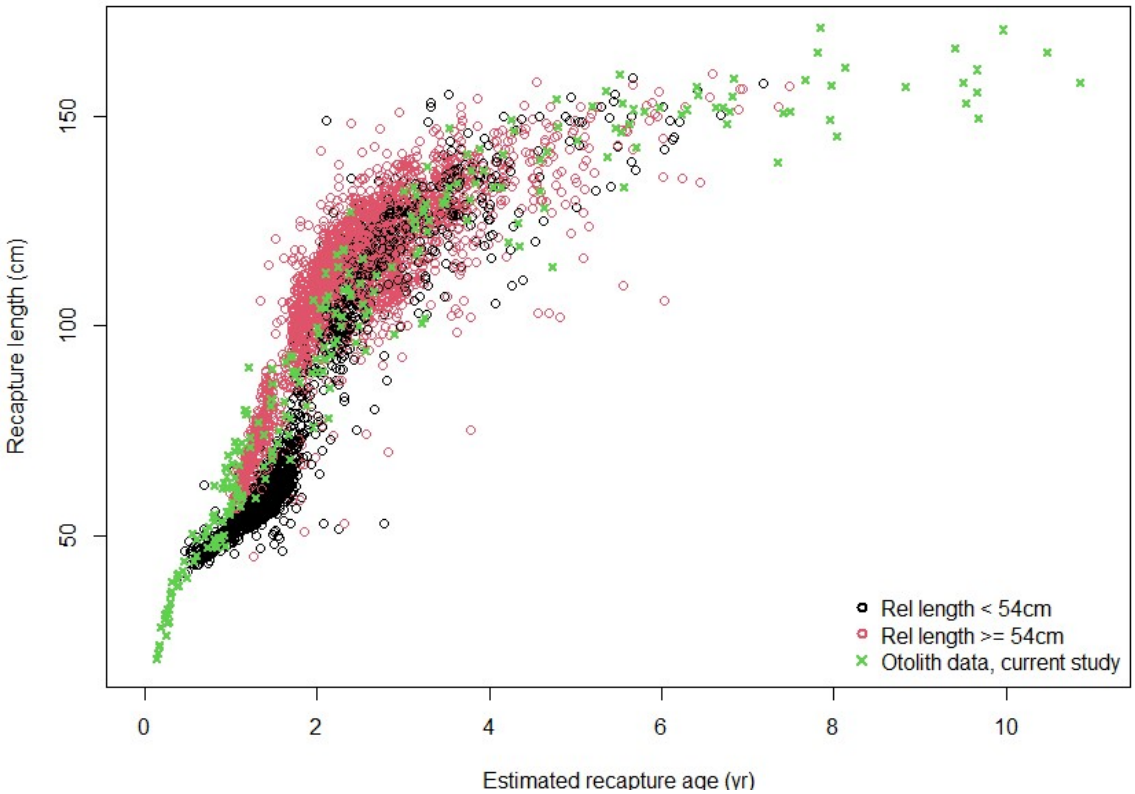

Figure 7. Recapture length versus recapture age as estimated for yellowfin tuna using release age derived from the length versus daily age relationship in Figure 5 plus the time at liberty. Data are colour-coded by release length (< 54 cm vs ≥54 cm). The otolith age and length data from the Farley et al. (2021a) are overlaid for comparison.

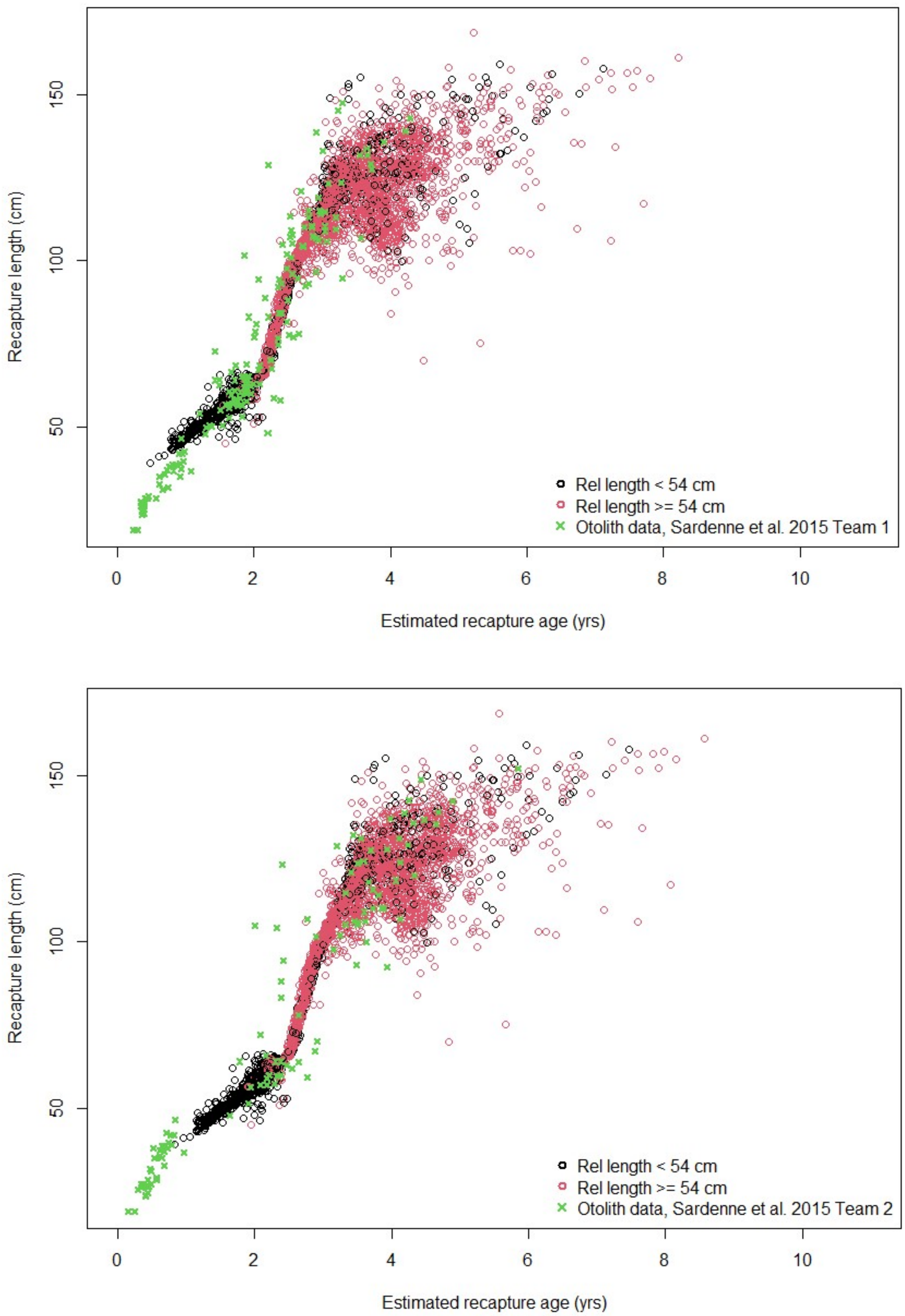

Figure 8. Recapture length versus recapture age as estimated for yellowfin tuna from the growth model in Eveson et al. (2015) which included tag-recapture data and otolith data from Sardenne et al. (2015) for reader Team 1 (top) or reader Team 2 (bottom). The otolith age and length data from Sardenne et al. (2015) for reader Team 1 (top) and reader Team 2 (bottom) are overlaid for comparison.

Figures – bigeye tuna

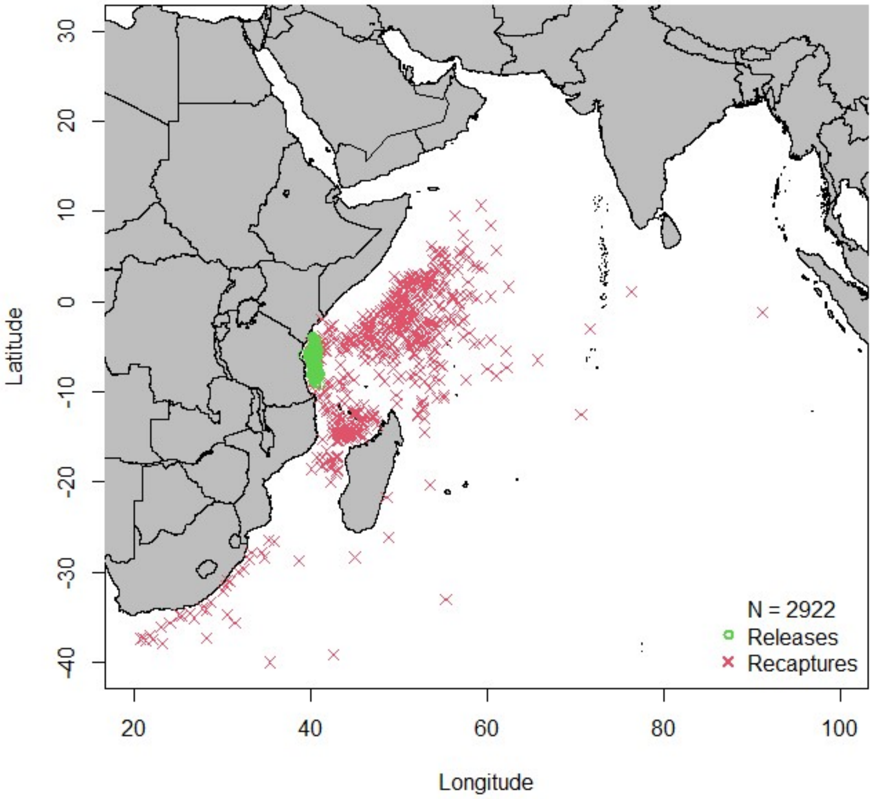

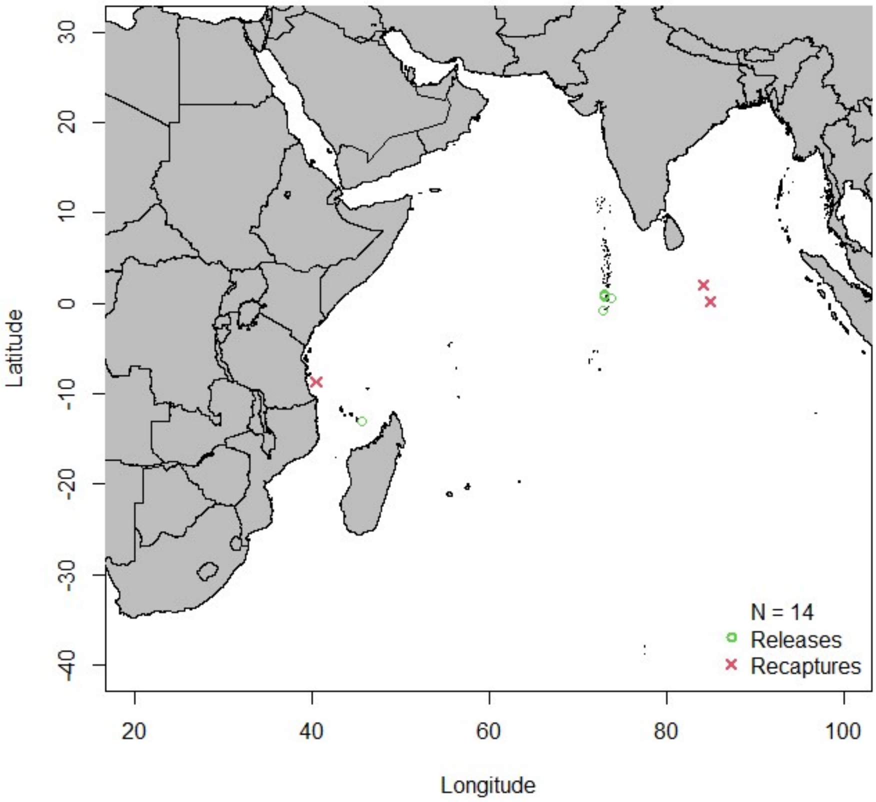

Figure 9. Map of the release and recapture locations for bigeye tuna used in the growth analysis of Eveson et al. (2015), showing fish that were released off Tanzania (top) and released elsewhere (bottom).

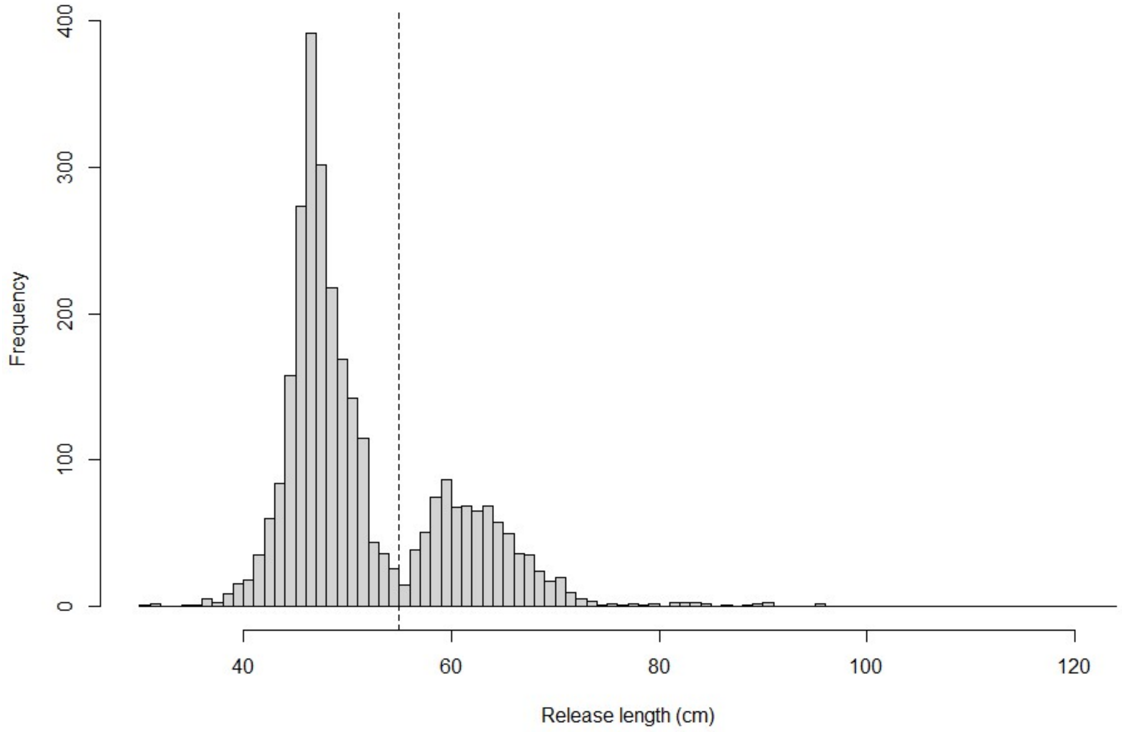

Figure 10. Release length distribution of bigeye tuna used in the growth analysis of Eveson et al. (2015). There is a separation between modes at 55 cm (dashed vertical line).

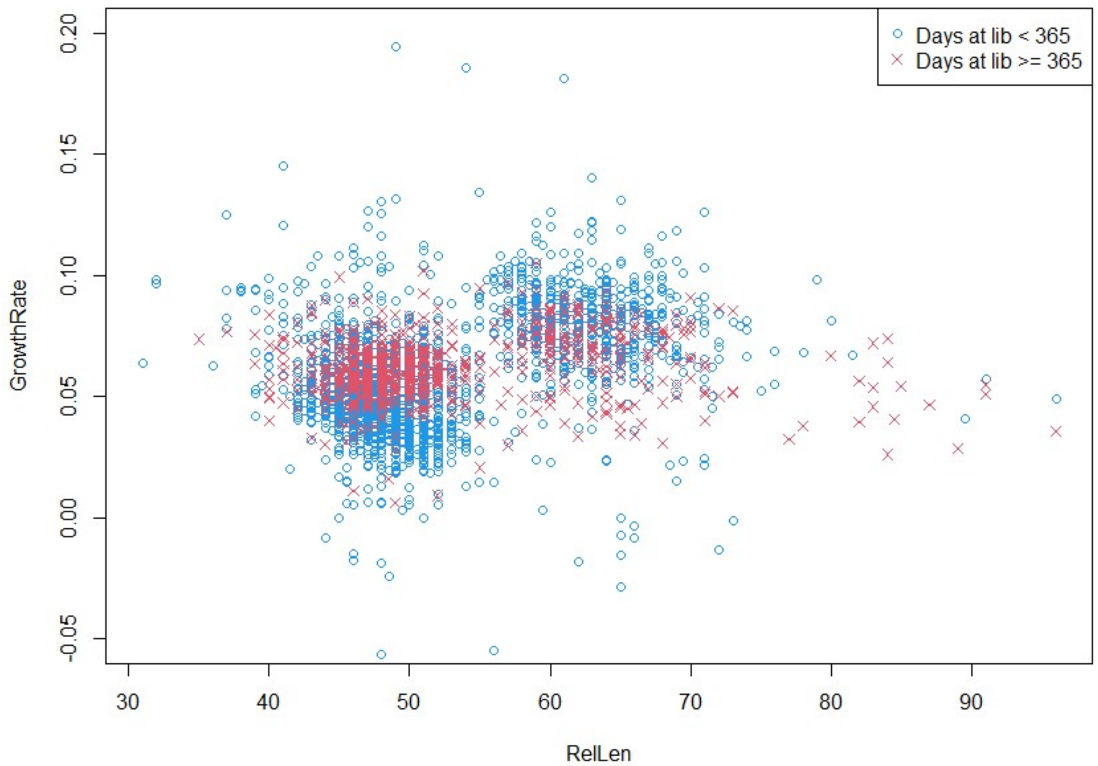

Figure 11. Growth rate (cm/day) versus release length (cm) for bigeye tuna, broken down by time at liberty (<365 days vs ≥365 days).

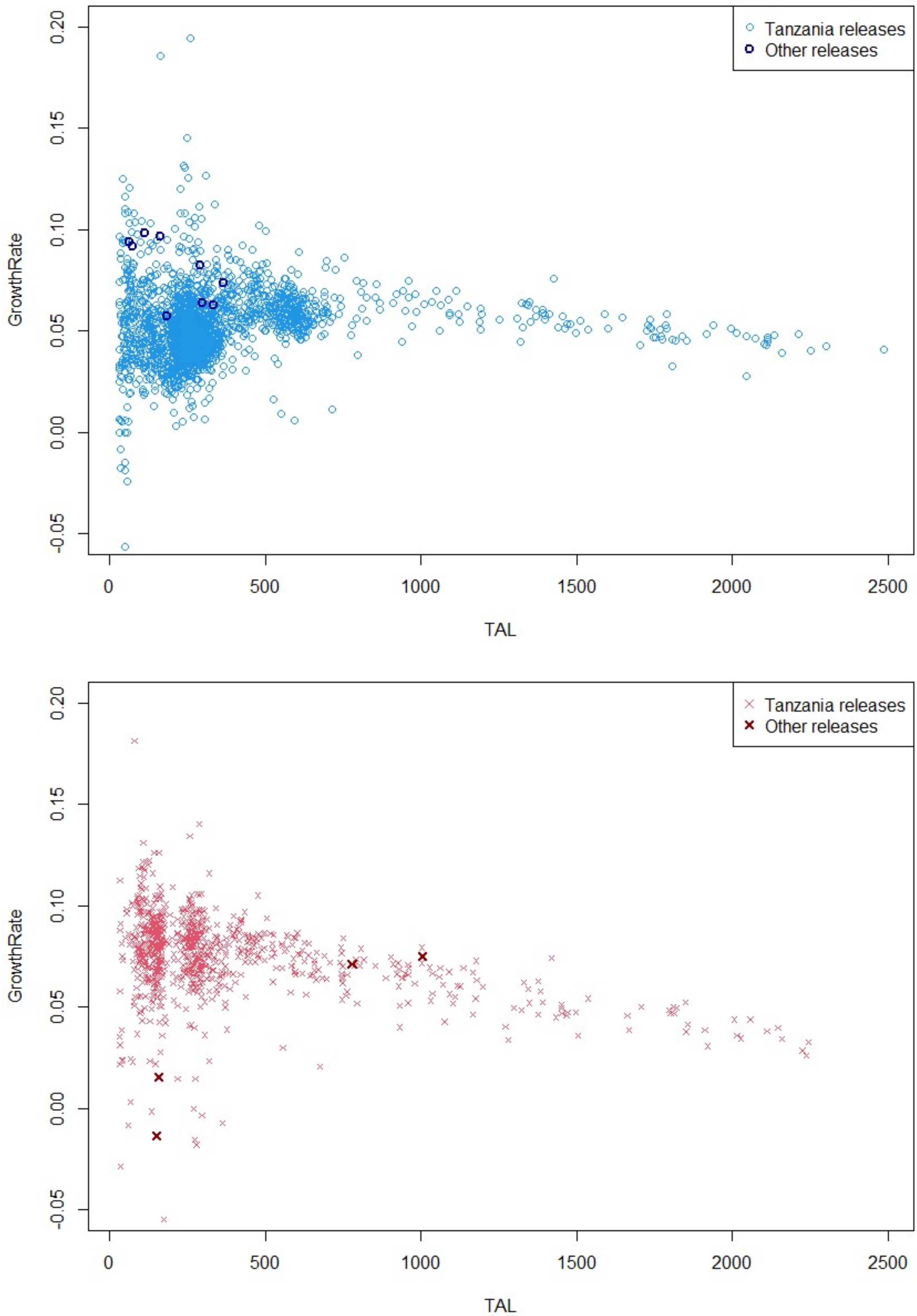

Figure 12. Growth rate (cm/day) versus time at liberty (TAL, days) for bigeye tuna that were <55 cm at release (top) and ≥55 cm at release (bottom). Those released in areas other than Tanzania are highlighted for comparison.

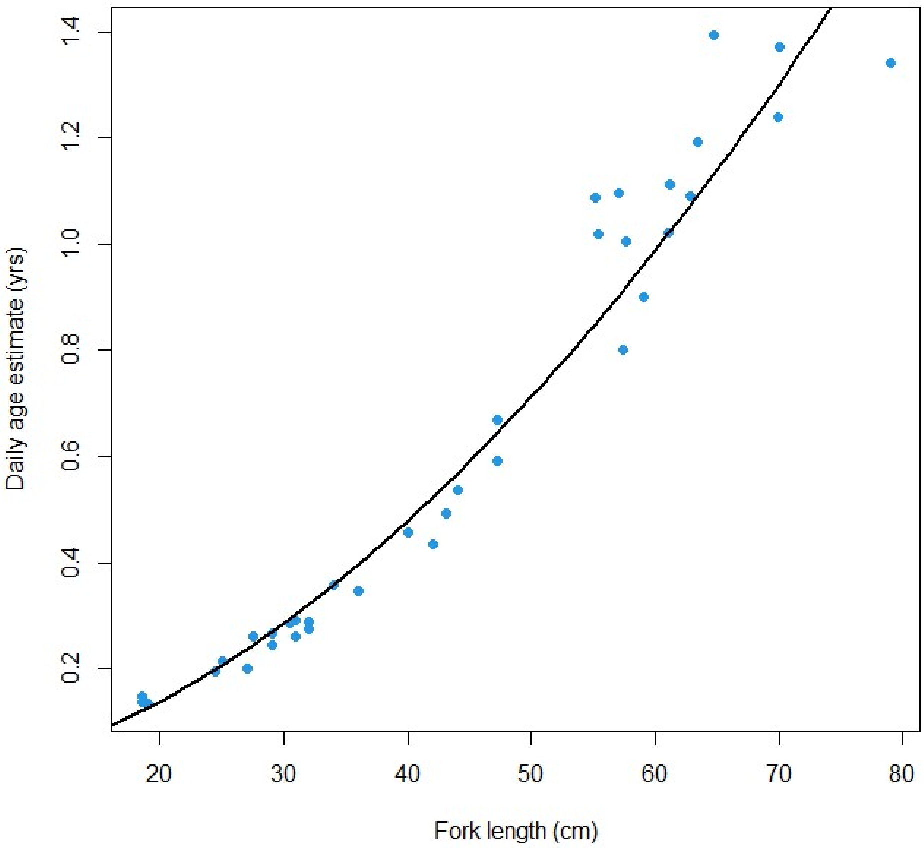

Figure 13. Fork length versus otolith daily age for bigeye tuna, with a power curve fitted to the data (taken from Farley et al. 2021b).

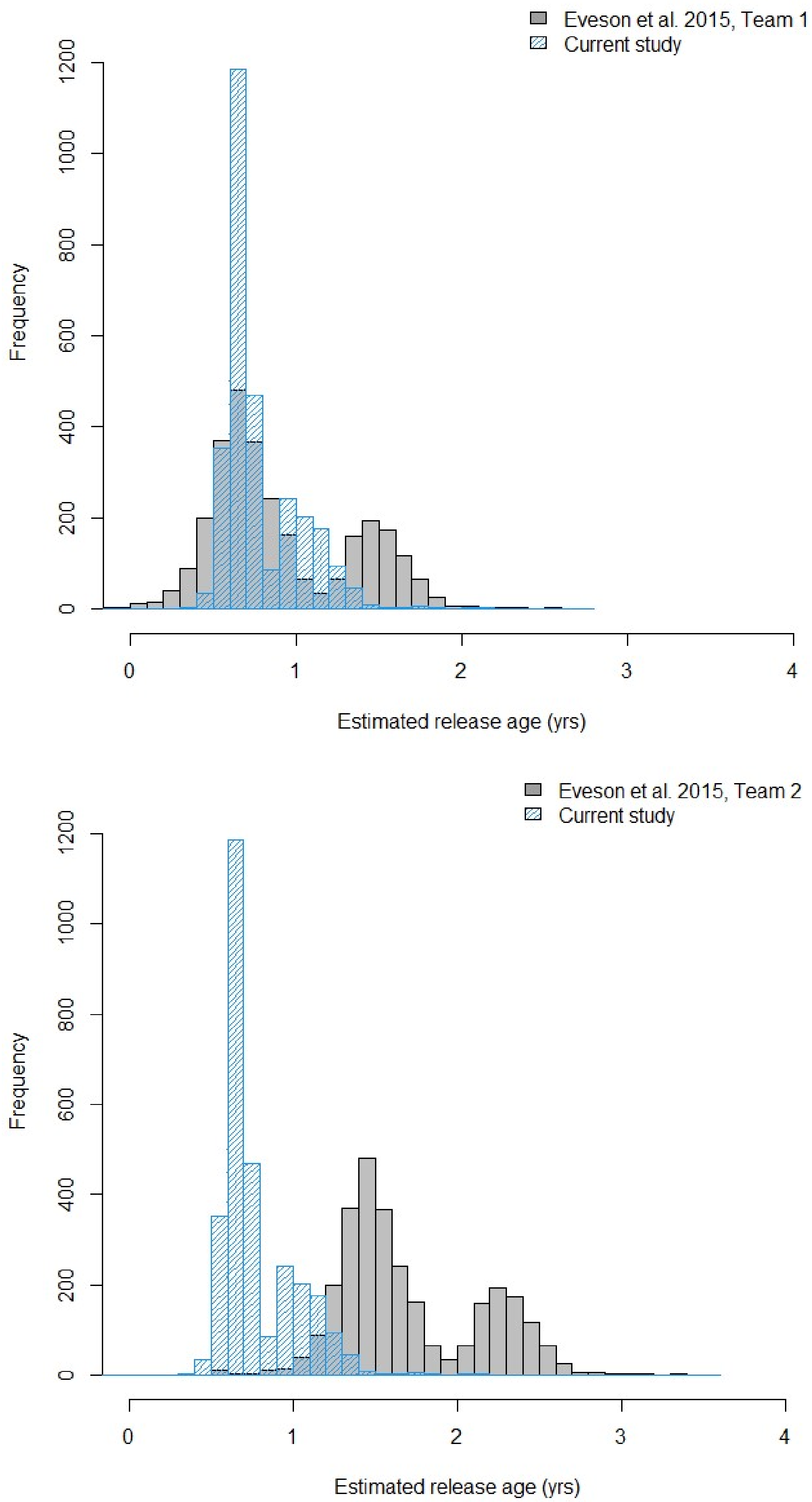

Figure 14. Histogram of release ages estimated for bigeye tuna in the current study using the length versus daily age relationship in Figure 5 (blue bars) compared to release ages estimated from the growth model in Eveson et al. (2015) (grey bars), which included tag-recapture data and otolith data from Sardenne et al. (2015) for reader Team 1 (top) or reader Team 2 (bottom).

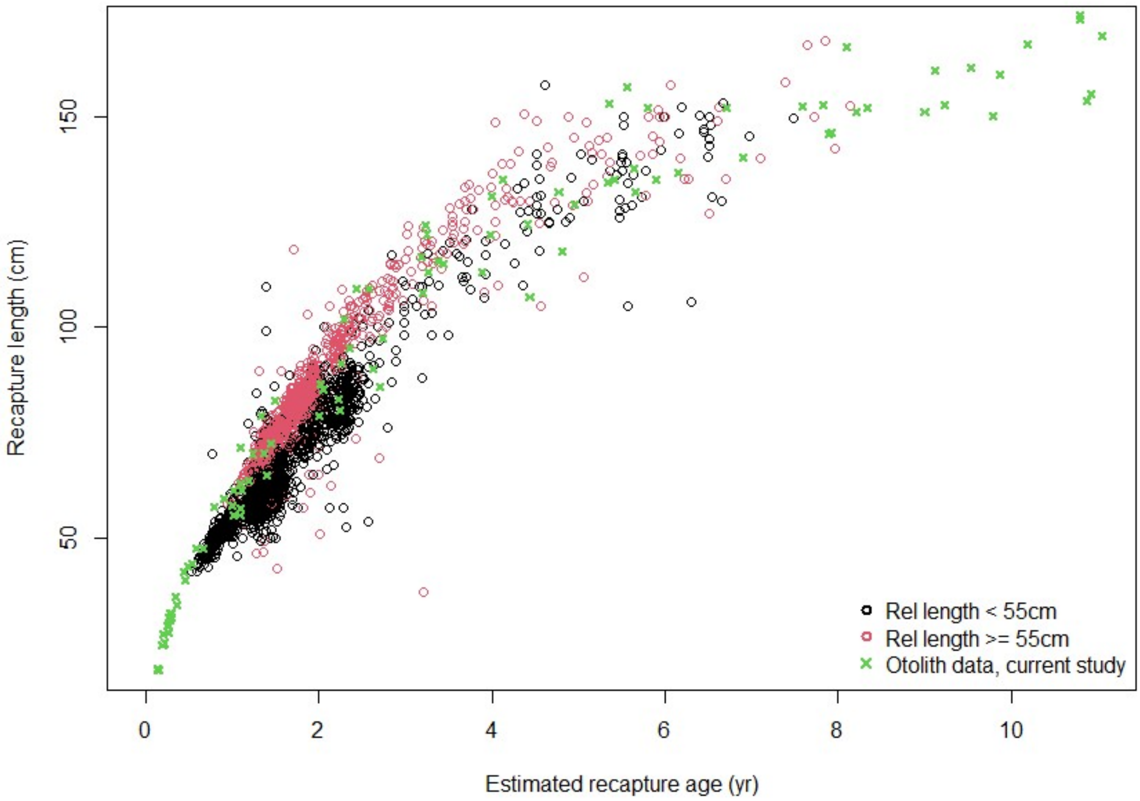

Figure 15. Recapture length versus recapture age as estimated for bigeye tuna using release age derived from the length vs daily age relationship in Figure 5 plus the time at liberty. Data are colour-coded by release length (< 54 cm vs ≥54 cm). The otolith age and length data from Farley et al. (2021b) are overlaid for comparison.

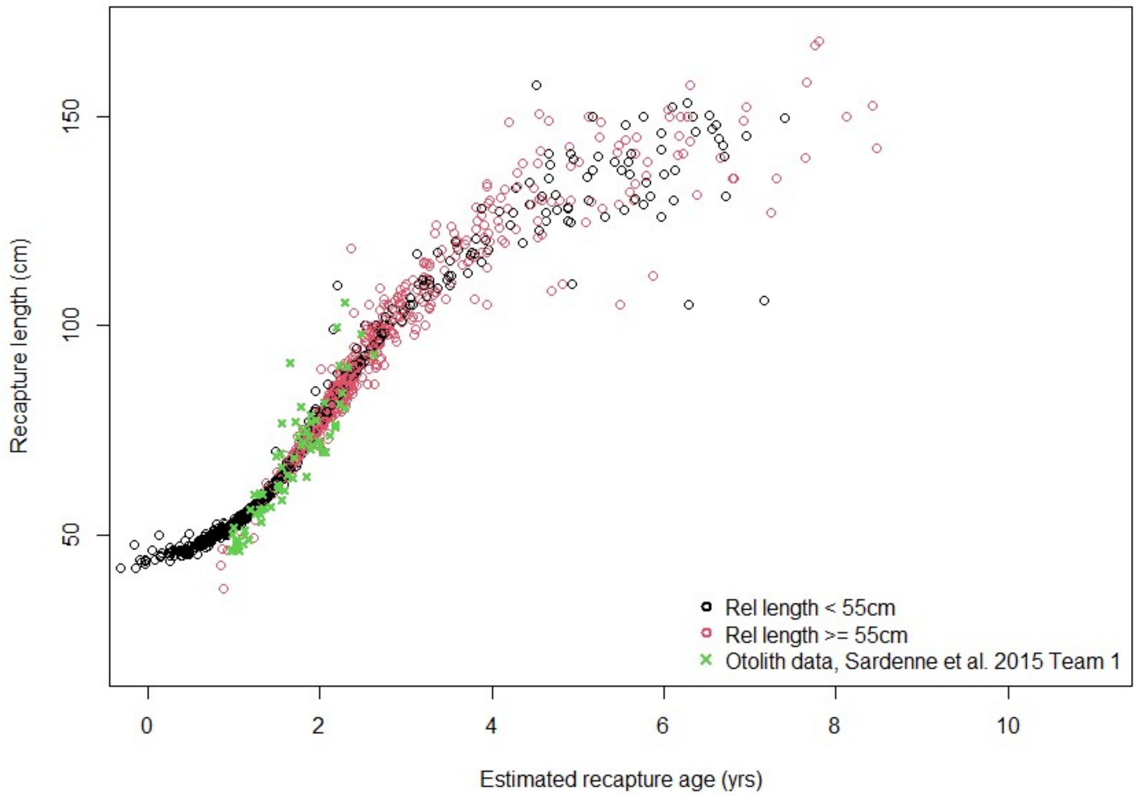

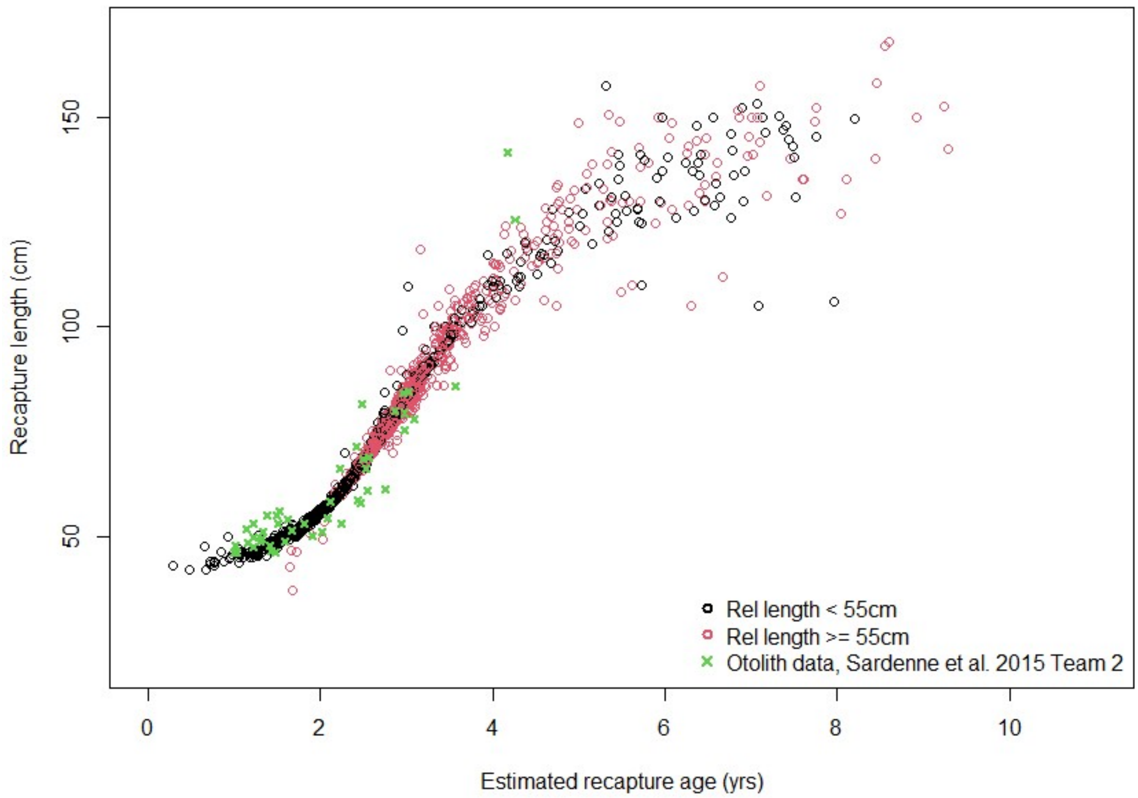

Figure 16. Recapture length versus recapture age as estimated for bigeye tuna from the integrated growth model in Eveson et al. (2015) using tag-recapture data and otolith data from Sardenne et al. (2015) for reader Team 1 (top) and reader Team 2 (bottom). The otolith age and length data from Sardenne et al. (2015) for reader Team 1 (top) and reader Team 2 (bottom) are overlaid for comparison.